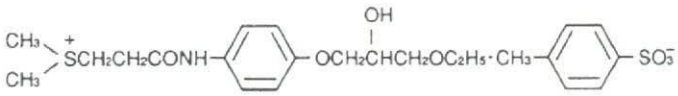

Fig. 1. Chemical structure of suplatast tosilate (IPD-1151T).

on the production of Th2 cytokines (IL-4, IL-5, and IL-13) in animal models of bronchial asthma (Iijima et al., 1999; Zhao et al., 2000; Matsumoto et al., 2002). Previous pharmacokinetics studies have shown that, after a single oral administration, suplatast tosilate is readily distributed into blood cells and stays in the cells with a half-life of 12 days, and an active bioavailability of suplatast tosilate in the lung tissue has also been confirmed (Kuwata et al., 1992). Based on these findings, it is possible that oral administration of suplatast tosilate may limit the development of pulmonary fibrosis through the inhibition of Th2 cytokines. To test this concept, the effects of suplatast tosilate on bleomycin-induced pulmonary fibrosis in C57BL/6 mice were investigated. The degree of pulmonary fibrosis was assessed by measuring the hydroxyproline content in the lungs, and the concentrations of Th2 cytokines, such as IL-4, IL-5, IL-6, and IL-13, in bronchoalveolar lavage (BAL) fluid were measured. In addition, the levels of MCP-1, a chemokine associated with Th2 polarization (Karpus et al., 1997; Gu et al., 2000; Matsukawa et al., 2000), and TGF-β, a cytokine strongly involved in the fibrogenic process, in BAL fluid were also assessed.

Materials and Methods

Animals. Specific pathogen-free, female C57BL/6 mice weighing 17 to 20 g were purchased from CLEA Japan (Tokyo, Japan). The animals were housed in pathogen-free rooms and maintained on laboratory chow, with free access to food and water. The committee on animal research at the University of Hiroshima approved all procedures.

Bleomycin Exposure. The mice were anesthetized with intraperitoneal pentobarbital, and the trachea was exposed through a cervical incision. Bleomycin (BLM; 1.5 mg/kg body weight; Nippon Kayaku, Tokyo, Japan) was dissolved in phosphate-buffered saline (PBS) and then instilled intratracheally with a 27-gauge needle.

Administration of Suplatast Tosilate. Suplatast tosilate (IPD-1151T; Fig. 1) was synthesized and supplied by the Taiho Pharmaceutical Co. Ltd. (Tokyo, Japan). The suplatast tosilate powder was dissolved in distilled water and administered into mice by oral gavage.

Experimental Protocol. After BLM was intratracheally administered, the mice were randomly divided into two groups, namely, the BLM + suplatast tosilate (ST) and BLM + distilled water (DW) groups. The mice of the BLM + ST group were given suplatast tosilate (100 mg/kg/day) by oral gavage daily until sacrificed, and the mice of the BLM + DW group received an equivalent volume of water. The control group received an equivalent volume of water after intratracheal PS administration. Animals were sacrificed 7, 14, and 21 days after BLM administration. Each group had eight mice at each time point. The control group (n = 8 mice) was sacrificed at 21 days after intratracheal instillation of PBS.

BAL and Cell Analysis. The mice were sacrificed with a lethal dose of pentobarbital, the trachea was cannulated with an 18-gauge needle, and the lungs were lavaged twice with 1 ml of PBS. The lavage fluids were pooled and were centrifuged at 300g for 10 min at 4°C. The supernatants were stored at −80°C for the measurement of cytokine concentrations. The cell pellets were resuspended in 1 ml of Dulbecco's modified Eagle's medium, and the total cell numbers were counted with a hemocytometer. Differential cell counts were determined by counting at least 300 cells on a smear prepared using cytospin (Thermo Fisher Scientific, Waltham, MA) and stained with Diff-Quick (Kokusai Shiyaku, Kobe, Japan).

Histopathology. The lung tissue specimens of the mice were fixed by inflation with a buffered 10% formalin solution. Lung tissue specimens were embedded in paraffin, and the sections were stained with hematoxylin and eosin (H&E) and thereafter were examined by light microscopy.

Cytokine Measurements. Commercially available ELISA kits for INF-γ, IL-4, IL-5, IL-6, IL-13, total and active TGF-β, and MCP-1 were obtained from R&D Systems (Minneapolis, MN). The concentration of each cytokine in the sample was measured following the manufacturer's protocols.

Hydroxyproline Assay. To assess lung fibrosis biochemically, lung tissues were homogenized and then analyzed for hydroxyproline content after acid hydrolysis, as described previously (Woessner, 1961). In brief, lung tissues were hydrolyzed with 12 N hydrochloric acid at 110°C for 24 h. After neutralization with sodium hydroxide, the hydrolysates were diluted with distilled water. Hydroxyproline in the hydrolysates was assessed colorimetrically at 550 nm for p-dimethylaminobenzaldehyde. The results were expressed as micrograms of hydroxyproline contained in total lung tissue.

Preparation of Alveolar Macrophages. Alveolar macrophages (AMs) were isolated as described previously, with slight modifications (Kaltreider et al., 1988). In brief, the mice were sacrificed with a lethal dose of pentobarbital, and the trachea was cannulated with an 18-gauge needle. The lungs were lavaged five times with 1 ml of PBS containing 0.1% EDTA. The lavage fluids were pooled and centrifuged at 300g for 10 min at 4°C. The cell pellet was washed once with PBS and resuspended in RPMI 1640 medium containing 10% fetal calf serum and 1% penicillin/streptomycin. The cells were plated at a cell density of 3×10^5 cells per well in 96-well plates, incubated for 45 min at 37°C in 5% CO_2, and gently washed three times with RPMI 1640 medium containing 10% fetal calf serum to remove unattached cells. Greater than 95% of the plastic-adherent cells obtained from normal mice and around 90% of the plastic-adherent cells obtained from BLM-injured mice were morphologically macrophages.

Assessment of MCP-1 Production in AMs. First, the cells adhering to the plastic were isolated from the mice intratracheally instilled with BLM 7 days before and then incubated in the presence or absence of suplatast tosilate at concentrations of 10 and 100 μg/ml. Twenty-four hours after the start of incubation with suplatast tosilate, the culture supernatants were collected and subjected for MCP-1 measurement. Next, the cells adhering to the plastic were isolated from normal mice. After preincubation with or without suplatast tosilate for 3 h, these cells were then incubated with lipopolysaccharide (LPS) at the concentration of 1 μg/ml in the presence or the absence of suplatast tosilate. Twenty-four hours after the addition of LPS, the culture supernatants were collected, and MCP-1 concentration was measured.

Statistics. The results are expressed as the mean ± S.E.M. Differences between treatment groups were analyzed using analysis of variance with Fisher's protected least significant difference test for pairwise comparisons (StatView; Abacus Concepts (Berkeley, CA). A p value of less than 0.05 was considered statistically significant.

Results

Effect of Suplatast Tosilate on BLM-Induced Pulmonary Fibrosis. To determine whether suplatast tosilate has an antifibrotic effect on the development of pulmonary fibrosis, mice were treated with suplatast tosilate after BLM was intratracheally instilled. Fourteen and 21 days after BLM administration, the lungs were excised, and collagen accumulation in the lungs was evaluated by measuring hydroxyproline content in the lungs. As shown in Fig. 2A, treatment with suplatast tosilate significantly suppressed the increase in the

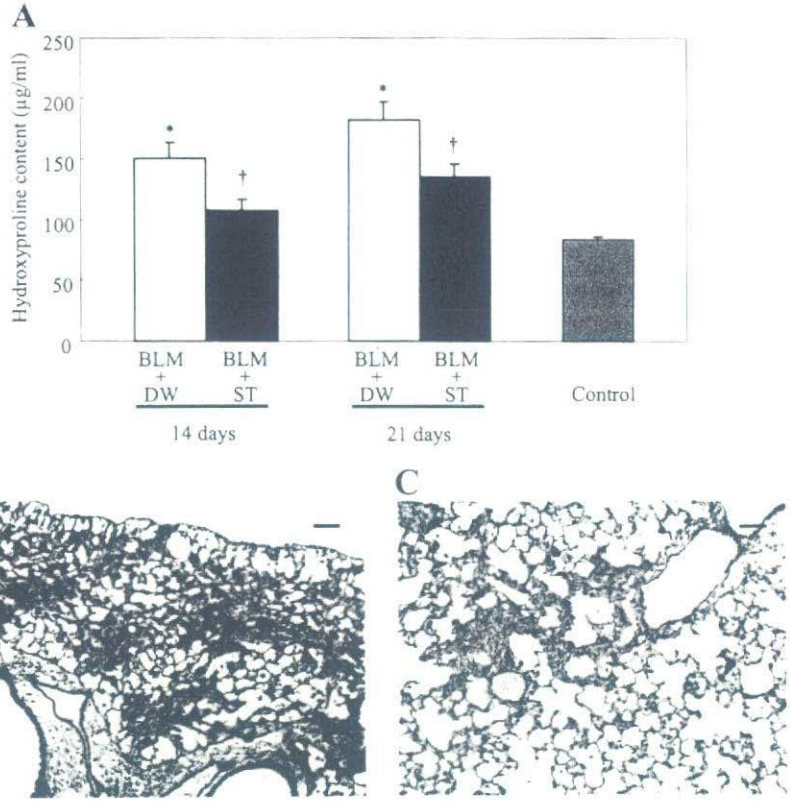

Fig. 2. Effect of suplatast tosilate on bleomycin-induced pulmonary fibrosis. After the intratracheal instillation of bleomycin (1.5 mg/kg), suplatast tosilate (100 mg/kg/day) or distilled water was administered daily to mice by oral gavage. A, fourteen and 21 days after the bleomycin administration, the lungs were excised, and hydroxyproline content in the lungs was measured. The increased amount of hydroxyproline after BLM induction was inhibited by suplatast tosilate. Data are shown as the mean ± S.E.M. for eight mice per group at each time point. *, $p < 0.05$ versus control group; †, $p < 0.05$ versus BLM + DW group. The lungs harvested at 21 days after the bleomycin administration were subjected to H&E staining. One representative example of four or five is shown for BLM + DW (B) and BLM + ST (C) groups. Internal scale bars, 50 μm.

collagen content in the lungs of the BLM-administered mice. To assess the histological changes, the lungs were excised, and the sections were stained with H&E at 21 days after BLM administration. The lesions with inflammation and fibrosis in the lungs of the BLM-administered mice treated with suplatast tosilate (Fig. 2C) significantly decreased in comparison with those in the lungs of the BLM-administered mice without suplatast tosilate treatment (Fig. 2B).

Effect of Suplatast Tosilate on BLM-Induced Lung Inflammation. To evaluate an effect of suplatast tosilate on the inflammatory responses induced by BLM, inflammatory cells recovered in the BAL fluids were analyzed 7, 14, and 21 days after intratracheal administration of BLM. The recovery rate of BAL fluid typically exceeded 85% and did not differ between the experimental groups. As shown in Fig. 3, the numbers of total inflammatory cells, macrophages, lymphocytes, and neutrophils in the BAL fluid were significantly elevated in the BLM-injected mice compared with the PBS-injected mice. Treatment with suplatast tosilate significantly decreased the number of total inflammatory cells, lympho-

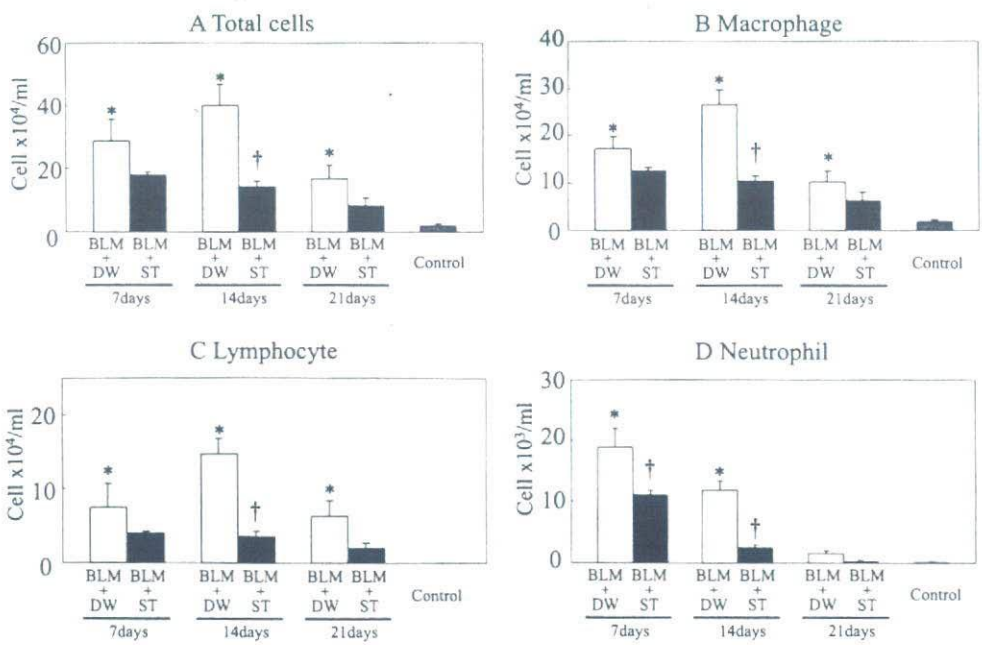

Fig. 3. Effect of suplatast tosilate on the cell analysis of BAL fluid in bleomycin-injured mice. After the intratracheal instillation of bleomycin (1.5 mg/kg), suplatast tosilate (100 mg/kg/day) or distilled water was administered daily to mice by oral gavage. BAL fluid specimens were obtained 7, 14, and 21 days after the bleomycin administration, and total cell counts and differential cell counts were performed. Data are shown as the mean ± S.E.M. for eight mice per group at each time point. *, $p < 0.05$ versus control group; †, $p < 0.05$ versus BLM + DW group.

cytes, and macrophages in the BAL fluid on day 14 and the number of neutrophils in the BAL fluid 7 and 14 days after BLM administration (Fig. 3).

Effect of Suplatast Tosilate on the Cytokine Levels in BAL Fluid from BLM-Injected Mice. To further analyze the effect of suplatast tosilate on the inflammatory responses induced by BLM, cytokine levels in the BAL fluid were measured 7, 14, and 21 days after the intratracheal administration of BLM. The concentrations of Th1 (INF-γ) and Th2 (IL-4, IL-5, IL-6, and IL-13) cytokines were first measured in the BAL fluid. The levels of INF-γ and IL-4 in the BAL fluids were found to be nearly equal to or lower than the minimal detectable limits for each ELISA system (data not shown). As a result, we omitted these two cytokines from the analysis. In comparison with the control mice, the levels of IL-5 and IL-13 in BAL fluid were not significantly elevated in BLM-injected mice except for IL-13 level on day 21, and treatment with suplatast tosilate did not change these levels (Fig. 4, A and C). In contrast, the intratracheal administration of BLM induced significant increases of IL-6 in BAL fluid, and treatment with suplatast tosilate significantly reduced the IL-6 level in BAL fluid 7 days after BLM administration (Fig. 4B). Thereafter, the levels of MCP-1, a chemokine associated with Th2 polarization, and total and active TGF-β, a cytokine strongly involved in fibrogenic process, were measured in the BAL fluid. The MCP-1 levels in the BAL fluid were significantly elevated in the BLM-injected mice in comparison with the PBS-injected mice 7 and 14 days after BLM administration, and, interestingly, treatment with suplatast tosilate was found to dramatically reduce these levels (Fig. 5A). The levels of total TGF-β in BAL fluid also significantly increased in the BLM-injected mice compared with PBS-injected mice 7, 14, and 21 days after BLM administration; however, treatment with suplatast tosilate did not decrease these levels in a statistically significant manner (Fig. 5B). Although their magnitudes were almost negligible in comparison with those of total TGF-β, the levels of active TGF-β in the BAL fluid were also significantly elevated in the BLM-injected mice in comparison with the PBS-injected mice at 7, 14, and 21 days after BLM administration. Interestingly, treatment with suplatast tosilate significantly reduced these levels at 14 and 21days after BLM administration (Fig. 5C).

Effect of Suplatast Tosilate on MCP-1 Production by AMs. MCP-1 has been found to be expressed in various type of cells including fibroblasts, endothelial cells, and mast cells; however, the major source of MCP-1 in the lungs of BLM-injected mice seems to be macrophages (Shen et al., 2005). Based on strong reduction of the MCP-1 level in the BAL fluid from BLM-injected mice treated with suplatast tosilate, it was possible that the suplatast tosilate had a direct effect on the MCP-1 production from AMs. We first evaluated the effect of suplatast tosilate on MCP-1 production from AMs isolated from BLM-injected mice (BLM-stimulated AMs). BLM-stimulated AMs in BAL fluid were collected 7 days after BLM administration and incubated with or without suplatast tosilate. As shown in Fig. 6A, the expression of MCP-1 in BLM-stimulated AMs decreased dose-dependently in the presence of suplatast tosilate. Thereafter, the effect of suplatast tosilate on MCP-1 production from naive AMs stimulated with inflammatory mediators was evaluated. LPS was chosen as an inflammatory mediator because a previous study demonstrated LPS

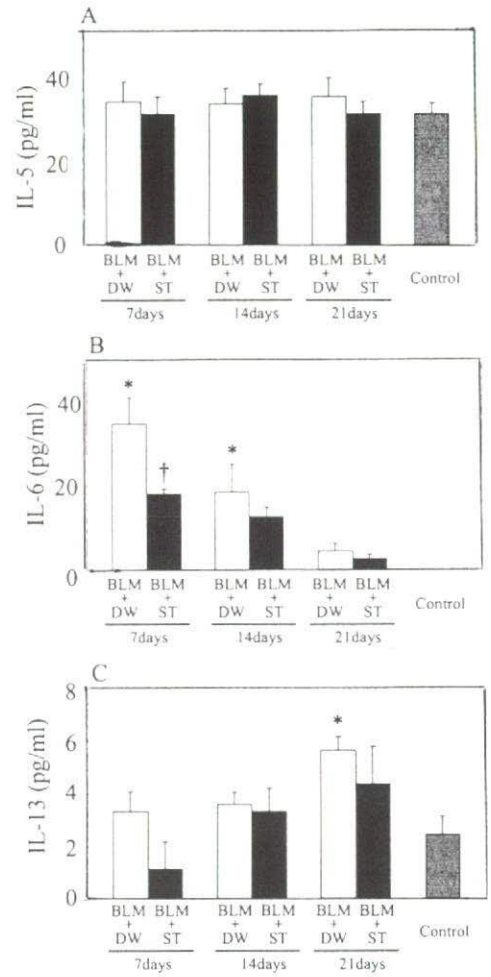

Fig. 4. Effect of suplatast tosilate on Th-2 cytokine levels in the BAL fluid from bleomycin-injured mice. After the intratracheal instillation of bleomycin (1.5 mg/kg), suplatast tosilate (100 mg/kg/day) or distilled water was administered daily to mice by oral gavage. BAL fluids were obtained 7, 14, and 21 days after the bleomycin administration. The concentrations of the cytokines in the BAL fluids were measured using commercially available ELISA kits. Note that IL-4 levels in the BAL fluid were nearly equal to or under the detectable limits of the ELISA kit; thus, the data for IL-4 were not shown. Data are shown as the mean ± S.E.M. for eight mice per group at each time point. *, $p < 0.05$ versus control group; †, $p < 0.05$ versus BLM + DW group.

to be the strongest inducer of MCP-1 expression in AMs (Brieland et al., 1995). Resident AMs in BAL fluid were collected from normal C57BL/6 mice and then were incubated with LPS in the presence or absence of suplatast tosilate. As shown in Fig. 6B, suplatast tosilate showed an inhibitory effect on the up-regulated production of MCP-1 from naive AMs stimulated with LPS.

Discussion

Suplatast tosilate is a novel antiallergic agent that is only available in Japan. This agent has been shown to possess an inhibitory effect on the production of Th2 cytokines (IL-4, IL-5, and IL-13) in animal models of bronchial asthma (Iijima et al., 1999; Zhao et al., 2000; Matsumoto et al., 2002). Based on these data, it is possible that suplatast tosilate might have an antifibrotic effect on an animal model of BLM-induced pulmonary fibrosis through the inhibition of Th2 cytokines. In the present study, the antifibrotic effect of suplatast tosi-

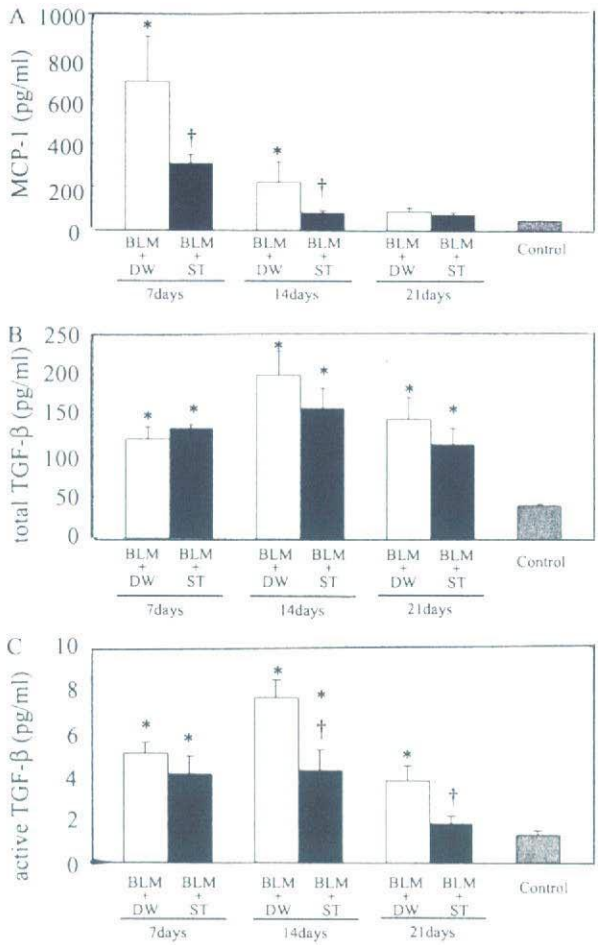

Fig. 5. Effect of suplatast tosilate on levels of MCP-1 and TGF-β in the BAL fluid from bleomycin-injured mice. After the intratracheal instillation of bleomycin (1.5 mg/kg), suplatast tosilate (100 mg/kg/day) or distilled water was administered daily to mice by oral gavage. BAL fluid specimens were obtained 7, 14, and 21 days after the bleomycin administration. The concentrations of MCP-1 (A) and total (B) and active (C) TGF-β in the BAL fluids were measured using commercially available ELISA kits. Data are shown as the mean ± S.E.M. for eight mice per group at each time point. *, $p < 0.05$ versus control group; †, $p < 0.05$ versus BLM + DW group.

late was demonstrated by the reduced hydroxyproline content in the lungs of BLM-injured mice treated with suplatast tosilate. Contrary to our hypothesis, however, an analysis of BAL fluids revealed that suplatast tosilate did not affect the concentrations of Th2 cytokines but significantly reduced MCP-1 levels. In addition, suplatast tosilate reduced the production of MCP-1 in AMs. Furthermore, suplatast tosilate was found to decrease the levels of IL-6 in BAL fluids from BLM-injured mice.

A most interesting finding of the current study is that the treatment of BLM-injured mice with suplatast tosilate was found to effectively suppress the increased MCP-1 levels in BAL fluids. In addition, suplatast tosilate also was able to reduce the production of MCP-1 in AMs. Although MCP-1, which is produced by various types of cells (Rollins, 1996; Boring et al., 1998), is an important chemoattractant for mononuclear cells, a relationship also has been clearly demonstrated between MCP-1 and the development of pulmonary fibrosis (Zhang et al., 1994). The MCP-1 levels in the sera and BAL fluids from IPF patients were also shown to be significantly higher than those in healthy subjects (Car et al., 1994; Suga et al., 1999). MCP-1 mRNA and protein are strongly expressed in epithelial cells, macrophages, and endothelial cells in the lungs of IPF patients (Antoniades et al., 1992; Iyonaga et al., 1994). In BLM-induced pulmonary fibrosis in rats, MCP-1 mRNA expression in lung tissue was significantly elevated between days 3 and 21 (Zhang et al., 1994). Moore et al. (2001) reported that the CC chemokine receptor 2 (receptor of MCP-1, MCP-3, and MCP-5 in mice)-deficient mice were protected from fluorescein isothiocyanate- and BLM-induced pulmonary fibrosis (Moore et al., 2001). Furthermore, anti-MCP-1 gene therapy blocking its signal transduction through CC chemokine receptor 2 was shown to attenuate the development of BLM-induced pulmonary fibrosis. In addition to its chemoattractant activity, MCP-1 is believed to possess direct profibrogenic effects because of its ability to stimulate fibroblast collagen expression (Gharaee-Kermani et al., 1996). Based on the observed close relationship between MCP-1 and pulmonary fibrosis, the antifibrotic effect of suplatast tosilate in BLM-induced pulmonary fibrosis thus can be considered to result from the suppression of MCP-1 expression in the lung. The expression of MCP-1 has been shown to be elevated on day 3 after BLM administration, whereas it persisted until day 21 (Zhang et al., 1994). In the present study, the MCP-1 levels in BAL fluid on day 7 after BLM administration dramatically increased and were still found to be significantly elevated on day 21 in the BLM-injured mice. Considering the expression pattern of MCP-1 in an animal model of BLM-induced pulmonary fibrosis, we believe that the treatment of the BLM-injured mice with suplatast tosilate, which started on the next day that BLM administration was begun and then continued daily until scarified, was necessary to elucidate the antifibrotic effect of suplatast tosilate mediated by the suppression of MCP-1.

In addition to MCP-1, the treatment of BLM-injured mice with suplatast tosilate significantly reduced the concentration of IL-6 in the BAL fluid 7 days after BLM administration. IL-6 is released by a variety of cells, including fibroblasts, and it has also been shown to mediate many inflammatory processes in the lung (Taga, 1997). In animal models, the lung-specific overexpression of IL-6 has been shown to produce lymphocytic alveolitis but little fibrosis (Denis, 1992; DiCosmo et al., 1994; Yoshida et al., 1995). Although in vitro studies have demonstrated the involvement of IL-6 in fibroblast proliferation, its role in fibrosis is still largely unknown (Knight et al., 2003). These previous reports suggest that IL-6 is an important proinflammatory cytokine to mediate the inflammatory processes in the lung, and the results of the present study demonstrated that suplatast tosilate has an anti-inflammatory effect through the suppression of IL-6.

Contrary to our original hypothesis, this study did not show suplatast tosilate to have an inhibitory effect on the production of Th2 cytokines in the model of BLM-induced pulmonary fibrosis using C57BL/6 mice. An analysis using commercially available ELISA kits revealed that the concentrations of IL-5 and IL-13 but not IL-4 in the BAL fluids from BLM-administered mice to be measurable. However, the levels of these cytokines were not significantly elevated in comparison with those of normal mice, thus indicating that the changes of Th2 cytokines in BAL fluids from BLM-injured

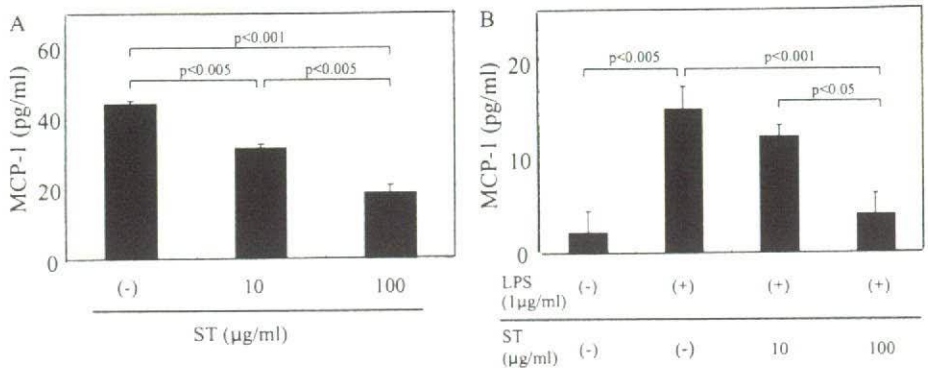

Fig. 6. Effect of suplatast tosilate on the production of MCP-1 in AMs. A, MCP-1 production in the AMs isolated from the mice intratracheally instilled with bleomycin. AMs were prepared as described under *Materials and Methods* and then incubated in the presence or absence of suplatast tosilate at concentrations of 10 and 100 μg/ml. Twenty-four hours after, the culture supernatants were collected and assayed for MCP-1. B, MCP-1 production in the LPS-stimulated AMs isolated from normal mice. AMs were prepared as described under *Materials and Methods*. After preincubation with or without suplatast tosilate for 3 h, these cells were then incubated with LPS at the concentration of 1 μg/ml in the presence or absence of suplatast tosilate. Twenty-four hours after the addition of LPS, the culture supernatants were collected and assayed for MCP-1.

C57BL/6 mice are very limited. In addition, suplatast tosilate did not affect the levels of Th2 cytokines in BAL fluids from BLM-administered C57BL/6 mice, in contrast to its successful suppression of Th2 cytokines in BAL fluids from a bronchial asthma model of Balb/C mice (Zhao et al., 2000). These data suggest that suplatast tosilate does not have an inhibitory effect on Th2 cytokines in BLM-induced pulmonary fibrosis. However, we believe that this conclusion is premature because the changes in the levels of these Th2 cytokines are too small in the BAL fluids obtained from BLM-injured mice.

Previous studies demonstrate that suplatast tosilate inhibits the release of the products of Th2 cells. Despite an extensive search for the molecular target of suplatast tosilate; however, the precise mechanism of the effect of suplatast tosilate is largely unknown. In the present study, the potential of suplatast tosilate to reduce the production of MCP-1 and IL-6 in the lung was demonstrated. Both MCP-1 and IL-6 are induced by the activation of nuclear factor κB. This suggests that the nuclear factor κB pathway may be a target of suplatast tosilate. However, further investigation is needed.

In conclusion, this study found that suplatast tosilate treatment limited the development of pulmonary fibrosis induced by BLM. Contrary to the original hypothesis, suplatast tosilate did not decrease the levels of Th2 cytokines in BAL fluids. However, suplatast tosilate significantly reduced the MCP-1 level in the BALF from BLM-treated mice. Suplatast tosilate was also found to reduce the production of MCP-1 in AMs. Considering that MCP-1 is a proinflammatory chemokine, which is strongly involved in the development of pulmonary fibrosis, these results suggest that suplatast tosilate has both anti-inflammatory and antifibrotic effects through the suppression of MCP-1 production in BLM-induced pulmonary fibrosis. In addition, the presence of constantly overexpressed MCP-1 in the lungs of IPF patients implies the possibility that suplatast tosilate also could potentially be used for the treatment of pulmonary fibrosis.

References

American Thoracic Society (2000) Idiopathic pulmonary fibrosis: diagnosis and treatment: international consensus statement: American Thoracic Society (ATS) and the European Respiratory Society (ERS). *Am J Respir Crit Care Med* **161**:646–664.

Antoniades HN, Neville-Golden J, Galanopoulos T, Kradin RL, Valente AJ, and Graves DT (1992) Expression of monocyte chemoattractant protein 1 mRNA in human idiopathic pulmonary fibrosis. *Proc Natl Acad Sci U S A* **89**:5371–5375.

Bajwa EK, Ayas NT, Schulzer M, Mak E, Ryu JH, and Malhotra A (2005) Interferon-gamma1b therapy in idiopathic pulmonary fibrosis: a metaanalysis. *Chest* **128**: 203–206.

Boring L, Gosling J, Cleary M, and Charo IF (1998) Decreased lesion formation in CCR2−/− mice reveals a role for chemokines in the initiation of atherosclerosis. *Nature* **394**:894–897.

Brieland JK, Flory CM, Jones ML, Miller GR, Remick DG, Warren JS, and Fantone JC (1995) Regulation of monocyte chemoattractant protein-1 gene expression and secretion in rat pulmonary alveolar macrophages by lipopolysaccharide, tumor necrosis factor-alpha, and interleukin-1 beta. *Am J Respir Cell Mol Biol* **12**:104–109.

Car BD, Meloni F, Luisetti M, Semenzato G, Gialdroni-Grassi G, and Walz A (1994) Elevated IL-8 and MCP-1 in the bronchoalveolar lavage fluid of patients with idiopathic pulmonary fibrosis and pulmonary sarcoidosis. *Am J Respir Crit Care Med* **149**:655–659.

Denis M (1992) Interleukin-6 in mouse hypersensitivity pneumonitis: changes in lung free cells following depletion of endogenous IL-6 or direct administration of IL-6. *J Leukoc Biol* **52**:197–201.

DiCosmo BF, Geba GP, Picarella D, Elias JA, Rankin JA, Stripp BR, Whitsett JA, and Flavell RA (1994) Airway epithelial cell expression of interleukin-6 in transgenic mice: uncoupling of airway inflammation and bronchial hyperreactivity. *J Clin Invest* **94**:2028–2035.

Furuie H, Yamasaki H, Suga M, and Ando M (1997) Altered accessory cell function of alveolar macrophages: a possible mechanism for induction of Th2 secretory profile in idiopathic pulmonary fibrosis. *Eur Respir J* **10**:787–794.

Gharaee-Kermani M, Denholm EM, and Phan SH (1996) Costimulation of fibroblast collagen and transforming growth factor beta1 gene expression by monocyte chemoattractant protein-1 via specific receptors. *J Biol Chem* **271**:17779–17784.

Gu L, Tseng S, Horner RM, Tam C, Loda M, and Rollins BJ (2000) Control of TH2 polarization by the chemokine monocyte chemoattractant protein-1. *Nature* **404**: 407–411.

Iijima H, Tamura G, Hsiue TR, Liu Y, Taniguchi H, and Shirato K (1999) Suplatast tosilate inhibits late response and airway inflammation in sensitized guinea pigs. *Am J Respir Crit Care Med* **160**:331–335.

Iyonaga K, Takeya M, Saita N, Sakamoto O, Yoshimura T, Ando M, and Takahashi K (1994) Monocyte chemoattractant protein-1 in idiopathic pulmonary fibrosis and other interstitial lung diseases. *Hum Pathol* **25**:455–463.

Kaltreider HB, Byrd PK, and Curtis JL (1988) Expression of Ia by murine alveolar macrophages is upregulated during the evolution of a specific immune response in pulmonary parenchyma. *Am Rev Respir Dis* **137**:1411–1416.

Karpus WJ, Lukacs NW, Kennedy KJ, Smith WS, Hurst SD, and Barrett TA (1997) Differential CC chemokine-induced enhancement of T helper cell cytokine production. *J Immunol* **158**:4129–4136.

King TE Jr, Safrin S, Starko KM, Brown KK, Noble PW, Raghu G, and Schwartz DA (2005) Analyses of efficacy end points in a controlled trial of interferon-gamma1b for idiopathic pulmonary fibrosis. *Chest* **127**:171–177.

Knight DA, Ernst M, Anderson GP, Moodley YP, and Mutsaers SE (2003) The role of gp130/IL-6 cytokines in the development of pulmonary fibrosis: critical determinants of disease susceptibility and progression? *Pharmacol Ther* **99**:327–338.

Kuwata T, Masuda H, Yamamoto Y, and Shindo T (1992) Pharmacokinetic studies of suplatast tosilate (IPD-1151T) (1): absorption, distribution and excretion after administration of ^{14}C-suplatast tosilate (IPD-1151T) to rats. *Drug Metab Pharmacokinet* **7**:399–421.

Matsukawa A, Hogaboam CM, Lukacs NW, Lincoln PM, Strieter RM, and Kunkel SL (2000) Endogenous MCP-1 influences systemic cytokine balance in a murine model of acute septic peritonitis. *Exp Mol Pathol* **68**:77–84.

Matsumoto K, Hayakawa H, Ide K, Suda T, Chida K, Hashimoto H, Sato A, and Nakamura H (2002) Effects of suplatast tosilate on cytokine profile of bronchoalveolar cells in allergic inflammation of the lung. *Respirology* **7**:201–207.

Moore BB, Paine R 3rd, Christensen PJ, Moore TA, Sitterding S, Ngan R, Wilke CA,

Kuziel WA, and Toews GB (2001) Protection from pulmonary fibrosis in the absence of CCR2 signaling. *J Immunol* **167**:4368–4377.

Raghu G, Brown KK, Bradford WZ, Starko K, Noble PW, Schwartz DA, and King TE Jr (2004) A placebo-controlled trial of interferon gamma-1b in patients with idiopathic pulmonary fibrosis. *N Engl J Med* **350**:125–133.

Rollins BJ (1996) Monocyte chemoattractant protein 1: a potential regulator of monocyte recruitment in inflammatory disease. *Mol Med Today* **2**:198–204.

Shen Y, Zhao HL, Du J, Li YT, Tan F, Huang CG, and Pei G (2005) Feitai, a Chinese herbal medicine, reduces transforming growth factor-beta1 and monocyte chemoattractant protein-1 expression in bleomycin-induced lung fibrosis in mice. *Clin Exp Pharmacol Physiol* **32**:1071–1077.

Suga M, Iyonaga K, Ichiyasu H, Saita N, Yamasaki H, and Ando M (1999) Clinical significance of MCP-1 levels in BALF and serum in patients with interstitial lung diseases. *Eur Respir J* **14**:376–382.

Taga T (1997) The signal transducer gp130 is shared by interleukin-6 family of haematopoietic and neurotrophic cytokines. *Ann Med* **29**:63–72.

Wallace WA, Ramage EA, Lamb D, and Howie SE (1995) A type 2 (Th2-like) pattern of immune response predominates in the pulmonary interstitium of patients with cryptogenic fibrosing alveolitis (CFA). *Clin Exp Immunol* **101**:436–441.

Woessner JF Jr (1961) The determination of hydroxyproline in tissue and protein samples containing small proportions of this imino acid. *Arch Biochem Biophys* **93**:440–447.

Yoshida M, Sakuma J, Hayashi S, Abe K, Saito I, Harada S, Sakatani M, Yamamoto S, Matsumoto N, and Kaneda Y (1995) A histologically distinctive interstitial pneumonia induced by overexpression of the interleukin 6, transforming growth factor beta 1, or platelet-derived growth factor b gene. *Proc Natl Acad Sci U S A* **92**:9570–9574.

Zhang K, Gharaee-Kermani M, Jones ML, Warren JS, and Phan SH (1994) Lung monocyte chemoattractant protein-1 gene expression in bleomycin-induced pulmonary fibrosis. *J Immunol* **153**:4733–4741.

Zhao GD, Yokoyama A, Kohno N, Sakai K, Hamada H, and Hiwada K (2000) Effect of suplatast tosilate (IPD-1151T) on a mouse model of asthma: inhibition of eosinophilic inflammation and bronchial hyperresponsiveness. *Int Arch Allergy Immunol* **121**:116–122.

Address correspondence to: Noboru Hattori, Department of Molecular and Internal Medicine, Graduate School of Biomedical Sciences, Hiroshima University, 1-2-3 Kasumi, Minami-ku, Hiroshima 734-8551, Japan. E-mail: nhattori@hiroshima-u.ac.jp

A Novel IκB Kinase-β Inhibitor Ameliorates Bleomycin-induced Pulmonary Fibrosis in Mice

Mami Inayama*, Yasuhiko Nishioka*, Momoyo Azuma, Susumu Muto, Yoshinori Aono, Hideki Makino, Kenji Tani, Hisanori Uehara, Keisuke Izumi, Akiko Itai, and Saburo Sone

Departments of Internal Medicine and Molecular Therapeutics, and Molecular and Environmental Pathology, Institute of Health Biosciences, University of Tokushima Graduate School, Tokushima; and Institute of Medicinal Molecular Design, Inc., Tokyo, Japan

Rationale: IκB kinase-β is a critical regulator in the activation of nuclear factor-κB (NF-κB), a transcription factor related to the expression and regulation of proinflammatory cytokines.
Objective: To evaluate if inhibition of IκB kinase-β ameliorates pneumonitis and pulmonary fibrosis.
Methods: We examined whether a novel IκB kinase-β inhibitor, IMD-0354, attenuates bleomycin-induced pulmonary fibrosis in mice.
Measurements and Main Results: Administration of IMD-0354 significantly improved the loss of body weight and survival of mice treated with bleomycin, whereas IMD-0354 alone did not cause any morphologic change in the lung. When mice were evaluated 28 d after bleomycin administration, IMD-0354 dose-dependently reduced the collagen content and fibrotic scores as shown by histologic examination. The findings in the bronchoalveolar lavage demonstrated that the proportions of neutrophils and lymphocytes were decreased in mice treated with IMD-0354 on Day 7 and 14, respectively. IMD-0354 treatment was confirmed to inhibit the activation of NF-κB, but not activator protein-1, in the lungs treated with bleomycin. The production of inflammatory cytokines tumor necrosis factor-α and interleukin-1β was reduced in the lungs of mice treated with IMD-0354.
Conclusions: These results suggest that IMD-0354 might be useful to ameliorate the inflammation in the lungs induced by fibrotic injury and the subsequent fibrogenesis via inhibiting the expression of profibrotic cytokines related to the activation of NF-κB.

Keywords: interleukin-1β; nuclear factor-κB, tumor necrosis factor-α

Idiopathic pulmonary fibrosis (IPF) is a progressive and lethal lung disease characterized by the proliferation of fibroblasts and deposition of extracellular matrixes (1, 2). Recent reports advocated the novel hypothesis that repeated alveolar epithelial injury and the subsequent abnormal wound healing, but not chronic inflammation, are critical events in the pathogenesis of pulmonary fibrosis, especially in IPF. However, they also indicated that inflammatory responses are likely to modulate and accelerate tissue injury and aberrant wound healing in lung fibrogenesis (2, 3). Besides, in other types of pulmonary fibrosis, including acute interstitial pneumonia and nonspecific interstitial pneumonia, acute or chronic inflammation is more closely related to lung fibrogenesis (4–6). Because the relationship between inflammation and fibrogenesis is not entirely clear, the targeted inhibition of lung inflammation can still be a potential therapy for pulmonary fibrosis.

To date, corticosteroids have been used for treatment of patients with pulmonary fibrosis, although their clinical effects are limited (1, 7). Because corticosteroids have various biological effects, which in turn frequently lead to serious side effects (7), there is a need for more selective approaches to inhibit lung inflammation that might reduce the subsequent fibrosis without adverse effects. On the basis of these concepts, targeted inhibition of nuclear factor-κB (NF-κB), which is a transcription factor related to the expression and regulation of proinflammatory cytokines, including tumor necrosis factor (TNF)-α and interleukin (IL)-1β, has been examined for its effects in reducing pulmonary fibrosis using the bleomycin model. Zhang and colleagues reported that administration of antisense oligonucleotides to NF-κB improved pulmonary fibrosis induced by bleomycin (8). However, Griesenbach and coworkers reported that intranasal inhalation of NF-κB decoy oligonucleotides failed to attenuate lung inflammation (9). These reports suggest that inhibition of NF-κB is a potential but not well established antifibrotic therapy.

The cytoplasmic binding of NF-κB to inhibitor of κB (IκB) prevents NF-κB activation. The serine phosphorylation of IκB allows its degradation by the 26S proteasome, and subsequently, NF-κB free of IκB translocates into the nucleus and activates gene transcription (10). There are two catalytic subunits of the IκB kinase (IKK) complex, IKKα and IKKβ (11, 12). IKKβ, but not IKKα, is required for TNF-α– and IL-1–mediated activation of NF-κB (13–15). Recently, it was reported that IKKβ is a critical target to inhibit the NF-κB pathway in alveolar macrophages because inhibition of NF-κB–inducing kinase, which functions upstream of the IKK complex, does not affect the production of NF-κB–related proinflammatory cytokines (16).

We therefore examined whether targeted inhibition of IKKβ reduced the pneumonitis/fibrosis induced by bleomycin in mice using a novel IKKβ inhibitor, IMD-0354. This article reports the profound antifibrotic effects of IMD-0354 achieved via inhibition of the production of profibrotic cytokines. Some of these studies have been previously reported in the form of abstracts (17).

METHODS

Detailed methods are described in the online supplement.

Mice and Materials

Eight-week-old C57BL/6 female mice were purchased from Charles River Japan, Inc. (Yokohama, Japan). Mice were maintained in the animal facility of the University of Tokushima under specific pathogen–free conditions according to the guidelines of our university (18). IMD-0354 (N-[3,5-bis-trifluoromethyl-phenyl]-5-chloro-2-hydroxy-benzamide; Figure 1) was kindly provided by the Institute of Medical Molecular Design (Tokyo, Japan). The specificity of IMD-0354 and the inhibitory activity for IKKβ were shown in Table E1 of the online supplement and previous reports (19, 20). Bleomycin was purchased from Nippon Kayaku Co. (Tokyo, Japan).

(Received in original form June 20, 2005; accepted in final form February 2, 2006)

Supported by grants from the Ministry of Health and Welfare and the Ministry of Education, Science, Sports, and Culture of Japan.

* M.I. and Y.N. are joint first authors and contributed equally to this work.

Correspondence and requests for reprints should be addressed to Saburo Sone, M.D., Ph.D., Department of Internal Medicine and Molecular Therapeutics, Institute of Health Biosciences, the University of Tokushima Graduate School, 3-18-15 Kuramoto-cho, Tokushima 770-8503, Japan. E-mail: ssone@clin.med.tokushima-u.ac.jp

This article has an online supplement, which is accessible from this issue's table of contents at www.atsjournals.org

Am J Respir Crit Care Med Vol 173. pp 1016–1022, 2006
Originally Published in Press as DOI: 10.1164/rccm.200506-947OC on February 2, 2006
Internet address: www.atsjournals.org

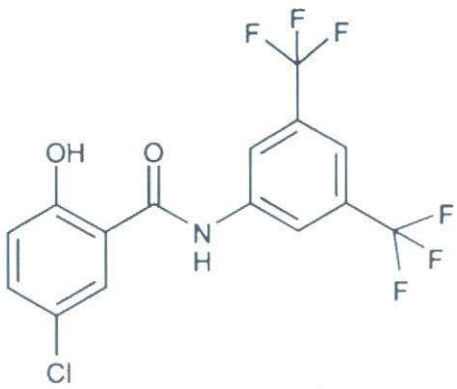

Figure 1. Chemical structure of IMD-0354.

Bleomycin Treatment

Osmotic minipumps (model 2001; Alza Pharmaceuticals, Palo Alto, CA) containing saline or bleomycin (125 or 150 mg/kg) were implanted subcutaneously (21, 22). Each experiment was performed in at least four mice per group.

Administration of IMD-0354

The IMD-0354 powder was dissolved in 0.5% carboxymethylcellulose (CMC; Sigma, Tokyo, Japan), and administered intraperitoneally into mice.

Bronchoalveolar Lavage

Bronchoalveolar lavage (BAL) was performed five times with saline (1 ml) using a soft cannula. After counting the cell number in the BAL fluid (BALF), cells were cytospun onto glass slides and stained with Diff-Quick (Baxter, Miami, FL) for cell classification.

Collagen Assay

The right lungs harvested on Day 28 were used for collagen assays. Total lung collagen was determined using the Sircol Collagen Assay kit (Biocolor Ltd., Belfast, Northern Ireland) according to the manufacturer's instructions (22).

Histopathology

The left lungs were fixed in 10% buffered formalin and embedded in paraffin. Sections (3–4 μm) were stained with hematoxylin and eosin. For the quantitative histologic analysis, a numeric fibrotic scale was used (Ashcroft score) (23). The mean score was considered the fibrotic score. Masson's trichrome staining was also performed.

Preparation of Nuclear Extracts

Preparation of nuclear extracts was performed using a CelLytic nuclear extraction kit (Sigma, Tokyo, Japan) according to the manufacturer's instructions (24). The nuclear extracts were kept at –80°C until use.

NF-κB and Activator Protein-1 ELISA

To evaluate the activation of NF-κB or activator protein-1 (AP-1), translocation of the p65 or c-Jun subunit into the nucleus was measured using a TransAM NF-κB p65 or c-Jun Transcription Factor Assay kit (Active Motif, Inc., Carlsbad, CA), respectively, according to the manufacturer's instructions (25). Results were determined by measuring the spectrophotometric absorbance at 655 nm and expressed as optical density (OD_{655}).

Electrophoretic Mobility Shift Assay

To confirm the activation of NF-κB, the electrophoretic mobility shift assay was performed as previously described (26). Nuclear protein

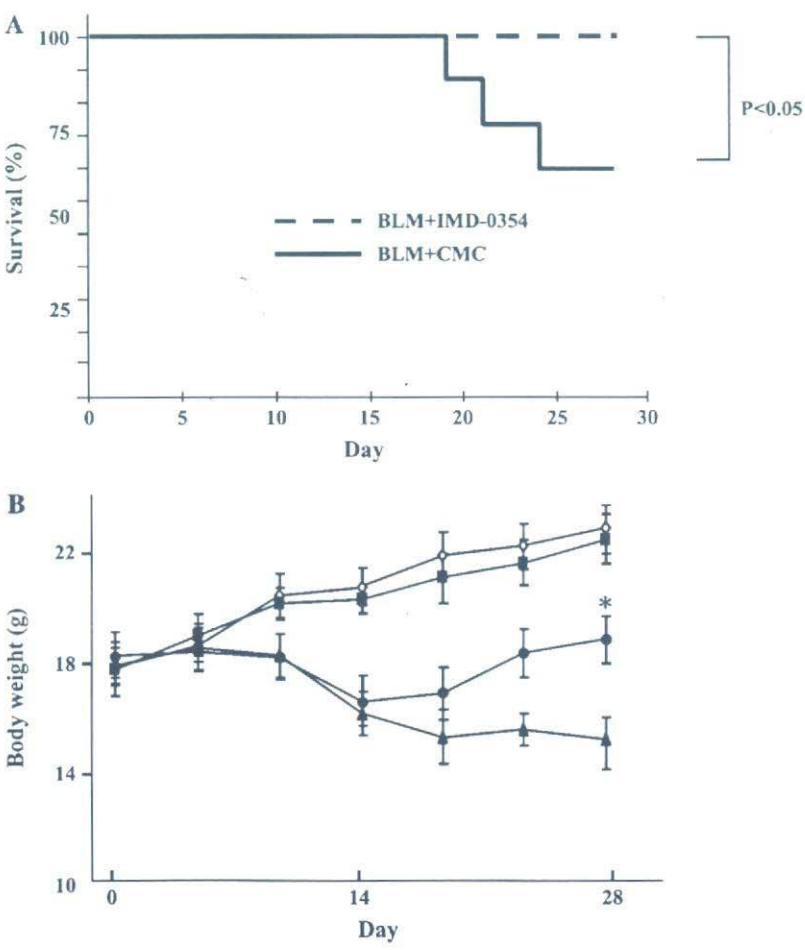

Figure 2. Effect of IMD-0354 on the survival rate and weight loss of mice treated with bleomycin. Mice were treated with 150 mg/kg of bleomycin (BLM). IMD-0354 (20 mg/kg) was given by intraperitoneal injection on a daily basis for the entire duration of the experiment (28 d). (*A*) The survival rates of mice treated with BLM alone (*solid line*, n = 16) or BLM + IMD-0354 (*dotted line*, n = 16) were examined. (*B*) The change in body weight of mice treated with saline alone (n = 10), IMD-0354 (n = 10), BLM alone (n = 16) or BLM + IMD-0354 (n = 16). Similar results were obtained in two separate experiments. *$p < 0.001$. CMC = carboxymethylcellulose. *Diamonds* = saline + CMC; *squares* = saline + IMD-0354; *triangles* = BLM + CMC; *circles* = BLM + IMD-0354.

extracts (5 μg) were incubated with a ^{32}P-labeled probe and loaded onto 5% polyacrylamide gels, and then electrophoresed and analyzed using an image analyzer (BAS 2000; Fuji Film Co., Tokyo, Japan).

ELISAs for TNF-α and IL-1β

The concentrations of murine TNF-α and IL-1β were quantified using ELISA kits (R&D Systems, Minneapolis, MN). The minimal detectable level of both TNF-α and IL-1β was 5.1 pg/ml.

Statistical Analysis

Comparisons among multiple groups were analyzed using the one-way analysis of variance with Newman-Keuls *post hoc* correction (GraphPad Prism, version 3.0; GraphPad Software, San Diego, CA). Differences were considered statistically significant if p values were less than 0.05.

RESULTS

IKKβ Inhibitor IMD-0354 Improves the Survival and Weight Loss Induced by Bleomycin

We first examined the *in vivo* effects of a novel IKKβ inhibitor, IMD-0354, on the survival and weight loss induced by bleomycin in mice. Mortality caused by bleomycin was dose dependent. Ten of 25 animals (40%) died from Day 16 to 24 after treatment with 150 mg/kg of bleomycin. The administration of 20 mg/kg/d of IMD-0354, however, significantly improved the survival rate of mice treated with bleomycin (Figure 2A). There were no deaths in the group of mice treated with both IMD-0354 and bleomycin.

The mice injected with bleomycin showed a significant loss of body weight from Day 14 as compared with those injected with saline, and weight loss did not recover until Day 28. In contrast, mice treated with both bleomycin and IMD-0354 (20 mg/kg/d) showed a significant weight loss on Day 14, but the weight partially recovered from Day 14 to 28 (Figure 2B). On Day 28, IMD-0354 significantly improved the weight loss caused by bleomycin ($p < 0.001$; Figure 2B), although mice in the group treated with both IMD-0354 and bleomycin still showed 15% weight loss on Day 28 as compared with the control group (saline + CMC). On the other hand, mice treated with saline + CMC or saline + IMD-0354 did not show any loss of body weight, indicating that 20 mg/kg/d of IMD-0354 was not toxic to mice.

Administration of IMD-0354 Ameliorates Bleomycin-induced Lung Fibrosis in Mice

To evaluate the antifibrotic effect of IMD-0354, mice were treated with 125 mg/kg of bleomycin and killed on Day 28. The fibrotic change in the lung was evaluated by histologic examination and measurement of total collagen content. As shown in Figure 3, administration of IMD-0354 alone did not generate any changes in lung morphology. However, when IMD-0354 was administered daily to bleomycin-treated mice, a significant reduction of fibrosis in the subpleural areas of lung was observed (Figure 3). These antifibrotic effects of IMD-0354 were also confirmed by histologic examination using the fibrotic score as described in METHODS (Figure 4B). The collagen assay demonstrated that treatment with IMD-0354 dose-dependently reduced the production of total collagen in bleomycin-treated lungs (Figure 4A). More than 5 mg/kg/d of IMD-0354 were effective in reducing the pulmonary fibrosis caused by bleomycin.

Next, we examined the effect of the treatment schedule using IMD-0354 on the bleomycin-induced pulmonary fibrosis. Mice were separately treated with IMD-0354 from Day 0 to 14 (early treatment) or Day 14 to 28 (late treatment). As shown in Figures 5A and 5B, reduction of the antifibrotic effect of IMD-0354, as indicated by the fibrotic score and collagen content, was observed in both groups, but neither groups showed a significant difference from the bleomycin-alone group.

Cell Analysis of BALF

Next, we analyzed the cells in BALF to evaluate the effect of IMD-0354 on the inflammatory responses induced by bleomycin. Administration of bleomycin elevated the number of inflammatory cells, including macrophages, lymphocytes, and neutrophils, on Days 7, 14, and 28. Analysis of cell classification also showed

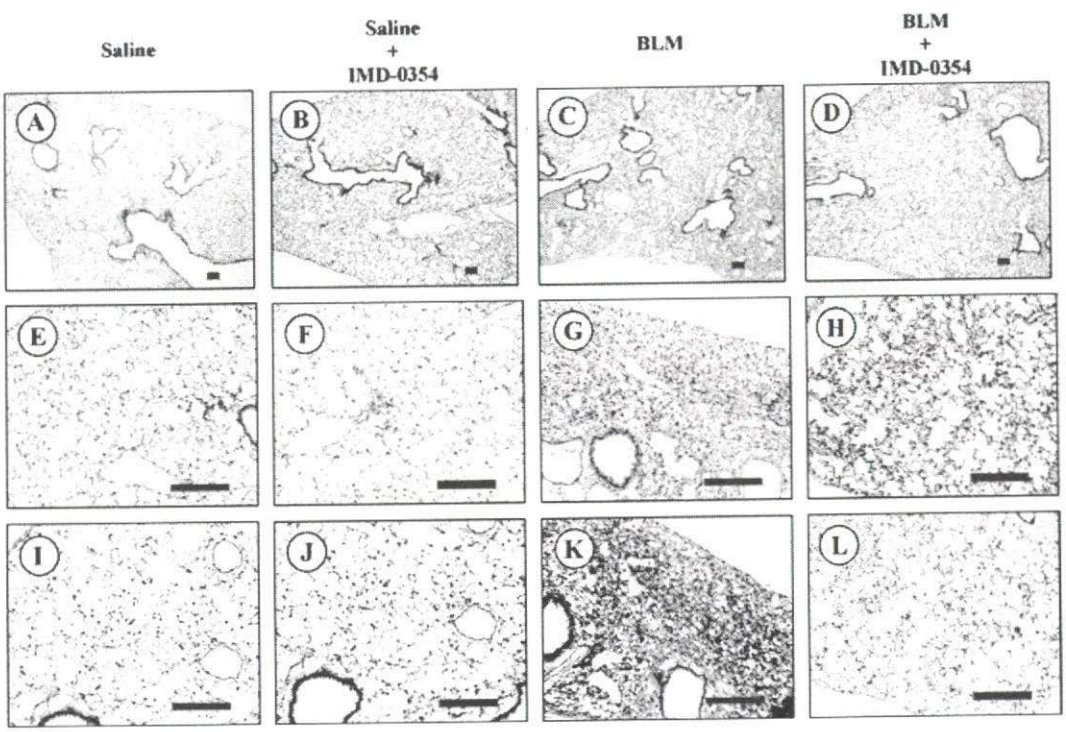

Figure 3. Histologic examination of the antifibrotic effects of IMD-0354 on BLM-induced pulmonary fibrosis. Mice were treated with osmotic minipumps containing saline or BLM (125 mg/kg). IMD-0354 (20 mg/kg) was given by intraperitoneal injection on a daily basis for the entire duration of the experiment. On Day 28, mice were killed and histologic examination was performed by hematoxylin and eosin (H&E) staining (*A–H*) and Masson's trichrome staining (*I–L*; original magnification: *A–D*, ×40; *E–L*, ×100). *A*, *E*, *I*: saline alone; *B*, *F*, *J*: saline + IMD-0354; *C*, *G*, *K*: BLM alone; *D*, *H*, *L*: BLM + IMD-0354. Data are representative of three separate experiments. *Bar* = 200 μm.

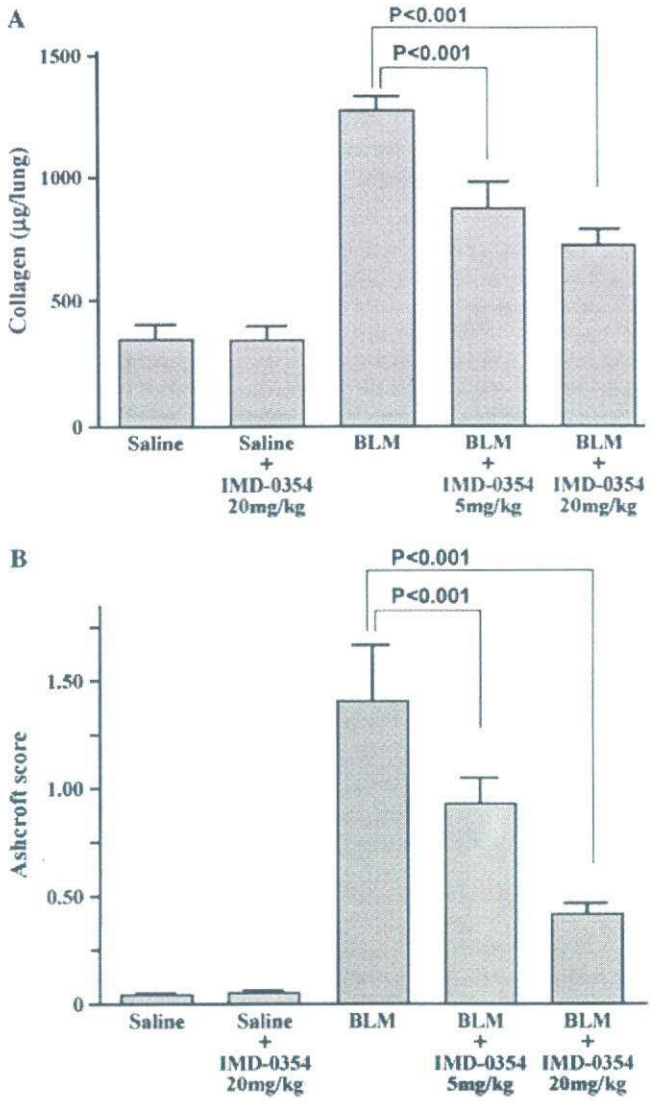

Figure 4. Quantitative examinations of the antifibrotic effects of IMD-0354 on BLM-induced pulmonary fibrosis. Mice were treated with osmotic minipumps containing saline or BLM. IMD-0354 (5 or 20 mg/kg) was given by intraperitoneal injection on a daily basis for the entire duration of the experiment. Mice were killed on Day 28. (*A*) Effects of IMD-0354 on collagen deposition after treatment with BLM. Collagen content in the right lung was measured using a Sircol collagen kit. Data are presented as mean ± SD of six mice. (*B*) Evaluation of fibrotic change in the lung using numeric fibrotic score. Histologic examination in the left lung was performed by H&E staining. The fibrotic score was determined by two pathologists as described in METHODS. Data are presented as mean ± SD of all fields examined in each group of six mice. Data are representative of two separate experiments.

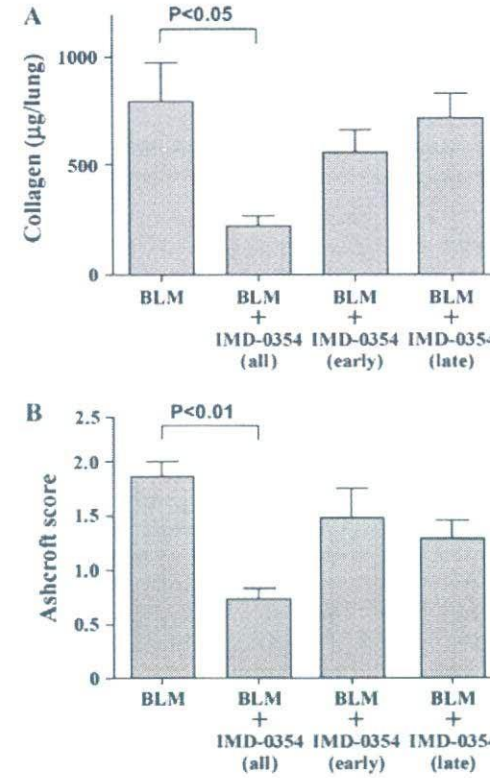

Figure 5. Effects of treatment schedule of IMD-0354 on the antifibrotic effects in BLM-induced pulmonary fibrosis. Mice were treated with osmotic minipumps containing saline or BLM. IMD-0354 (20 mg/kg/d) was injected intraperitoneally from Day 0 to 14 (early treatment) or Day 14 to 28 (late treatment). Mice were killed on Day 28. (*A*) Effects of IMD-0354 on collagen deposition after treatment with BLM. Collagen content in the right lung was measured using a Sircol collagen kit. Data are presented as mean ± SD of eight mice. (*B*) Evaluation of fibrotic change in the lung using numeric fibrotic score. Histologic examination in the left lung was performed by H&E staining. The fibrotic score was determined by two pathologists as described in METHODS. Data are presented as mean ± SD of all fields examined in each group of eight mice. Data are representative of three separate experiments.

that bleomycin treatment enhanced the percentage of lymphocytes and neutrophils on Days 7, 14, and 28. Administration of IMD-0354 significantly reduced the percentage of neutrophils and lymphocytes in BALF on Days 7 and 14, respectively (Table 1).

Inhibition of Activation of NF-κB by IMD-0354

To confirm the inhibition of activation of NF-κB by IMD-0354, we used a p65 ELISA to examine the amount of p65 subunit of NF-κB in the nuclear fraction of lung tissues and BALF of bleomycin-treated mice with or without IMD-0354. Bleomycin induced the maximal nuclear translocation of p65 of NF-κB on Day 7 (data not shown). The treatment with IMD-0354 significantly inhibited the nuclear translocation of p65 subunit in both lung tissues and BALF (Figures 6A and 6B). On the other hand, the activation of AP-1, defined by the nuclear translocation of c-Jun subunit, was not inhibited by IMD-0354 (Figures 6C and 6D). Furthermore, an electrophoretic mobility shift assay showed that the DNA binding activity of NF-κB significantly decreased in nuclear extracts of the lungs in mice treated with both bleomycin and IMD-0354 as compared with bleomycin alone (Figure 6E), and that the positive bands disappeared by the addition of an excess of the unlabeled NF-κB oligonucleotides (Figure 6F).

IMD-0354 Inhibits the Expression of TNF-α and IL-1β in Bleomycin-treated Lung

We examined whether IMD-0354 inhibited the expressions of TNF-α and IL-1β, which is regulated by the activation of NF-κB, in homogenates and BALF of lungs treated with bleomycin. TNF-α was detected 3 to 7 d after the injection of bleomycin (data not shown). IMD-0354 reduced the level of TNF-α in both lung homogenates and BALF (Figures 7A and 7B). There was a

TABLE 1. ANALYSIS OF BRONCHOALVEOLAR LAVAGE

Days after Treatment	Total Cells ($\times 10^6$)	Cell Differentiation (%)		
		Macrophages	Lymphocytes	Neutrophils
Day 0	0.69 ± 0.14	94.8 ± 2.2	3.2 ± 1.8	2.1 ± 0.3
Day 7				
BLM	2.20 ± 0.57	63.2 ± 11.4	6.38 ± 4.82	30.18 ± 8.53
BLM + IMD-0354	1.33 ± 0.33	96.9 ± 2.22	0.55 ± 0.34	2.55 ± 2.17*
Day 14				
BLM	6.36 ± 2.91	67.2 ± 10.20	24.7 ± 7.68	8.05 ± 3.65
BLM + IMD-0354	6.58 ± 2.42	78.3 ± 4.98	4.98 ± 3.09*	16.63 ± 5.15
Day 28				
BLM	2.19 ± 0.79	61.01 ± 5.10	28.68 ± 3.75	10.30 ± 4.69
BLM + IMD-0354	3.00 ± 1.64	65.75 ± 6.53	24.30 ± 3.59	9.95 ± 3.66

Definition of abbreviation: BLM = bleomycin.

Mice were treated with osmotic minipumps containing BLM (125 mg/kg). IMD-0354 (20 mg/kg) was intraperitoneally injected daily. On Days 0, 7, 14, and 28, bronchoalveolar lavage was performed as described in METHODS. Data are presented as mean ± SD in the group of six mice. Similar results were obtained in three separate experiments.

* $p < 0.001$ versus percentage in BLM group.

significant difference in the level of TNF-α in BALF between the groups of bleomycin alone and bleomycin + IMD-0354 (8.3 ± 1.7 vs. 2.9 ± 1.5 pg/ml, $p < 0.001$) and in lung homogenates between these groups (44.2 ± 14.5 vs. 19.0 ± 5.8 pg/ml, $p < 0.001$). The level of IL-1β in BALF was below the limit of sensitivity at all time points (data not shown). However, IL-1β was detected in the lung tissue homogenates from mice treated with bleomycin. The level of IL-1β in mice treated with bleomycin + IMD-0354 was significantly lower than that in mice treated with bleomycin alone (46.4 ± 22.7 vs. 90.6 ± 18.9 pg/ml, $p < 0.05$; Figure 7C).

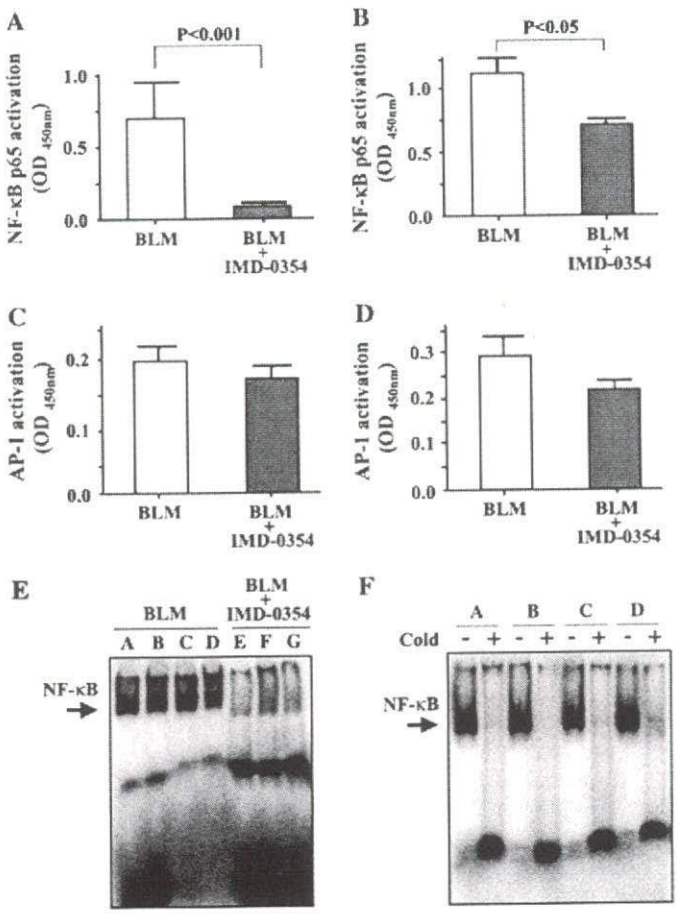

Figure 6. Inhibition of activation of nuclear factor (NF)-κB, but not activated protein (AP)-1, by IMD-0354 in the lungs treated with BLM. NF-κB activities in nuclear protein extracts of bronchoalveolar lavage fluid (BALF; *A*) and lung tissues (*B*) in mice treated with BLM with or without IMD-0354 on Day 7 were examined by measuring the level of the p65 subunit of NF-κB heterodimer using a trans AM kit (Active Motif, Inc., Carlsbad, CA). AP-1 activity was also examined in BALF (*C*) and lung tissues (*D*) by measuring the level of the c-Jun subunit of AP-1 heterodimer using a trans-AM kit. Data are presented as mean ± SD of four mice. The DNA binding activity of NF-κB in nuclear extracts of lung tissues was examined by an electrophoretic mobility shift assay (*E*). Competition experiments were performed by adding a 1,000-fold excess of unlabeled oligonucleotide before the labeled probes (*F*). Each *lane* in *E* and *F* shows the data from the nuclear extract of the lung of an individual mouse. Data are representative of two separate experiments.

DISCUSSION

The present study demonstrated that a novel IKKβ inhibitor, IMD-0354, effectively prevented bleomycin-induced pulmonary fibrosis via inhibition of the activation of NF-κB in the lungs. The analysis of BALF indicated that the antifibrotic effects of IMD-0354 were at least in part mediated by reducing the accumulation of neutrophils and lymphocytes in the lungs and the profibrotic cytokines TNF-α and IL-1β.

The antiinflammatory effects of corticosteroids, which have been used for the therapy for pulmonary fibrosis, are mediated by various mechanisms that lead to several adverse events, including diabetes mellitus, osteoporosis, peptic ulcers, and so on (27, 28). Therefore, antifibrotic therapy targeting the activity of NF-κB might have the potential to reduce serious side effects as well as enhance the antiinflammatory and antifirotic effects. Recently, Zhang and coworkers showed the antifibrotic effects of antisense oligonucleotides to NF-κB, whereas the inhibition of NF-κB in lung homogenates was not achieved (8). Griesenbach and colleagues reported that NF-κB decoy oligonucleotides failed to inhibit lung inflammation induced by bleomycin because oligonucleotides administered intranasally did not reach the nuclei of lung tissue cells (9). These reports suggest that antifibrotic

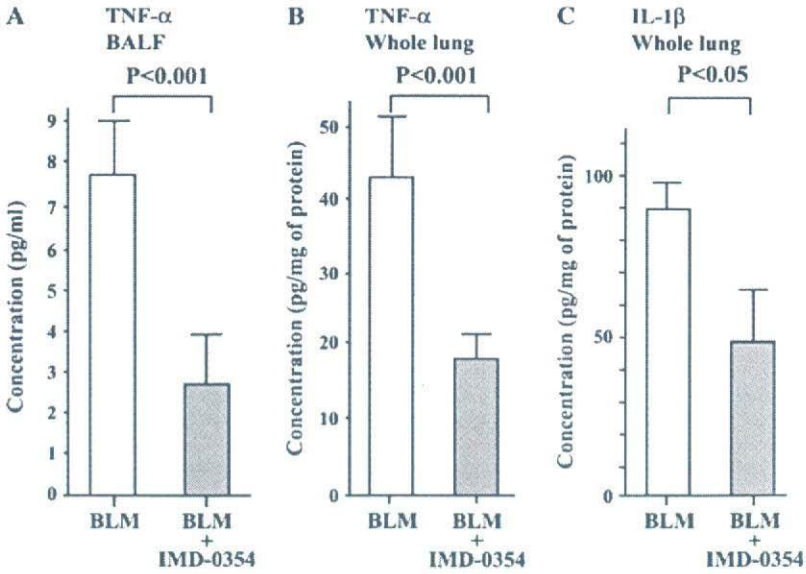

Figure 7. IMD-0354 inhibits the expression of tumor necrosis factor (TNF)-α and interleukin (IL)-1β in BALF or lung homogenates of mice treated with BLM. The levels of TNF-α and IL-1β in BALF and lung homogenates 7 d after treatment with BLM were measured by ELISA as described in METHODS. Data are shown as the mean ± SD of eight mice. Data are representative of two separate experiments.

effects of oligonucleotides inhibiting the activity of NF-κB are still controversial.

In contrast to the previous findings, we clearly demonstrated here the successful inhibition of NF-κB, but not AP-1, in lung homogenates by systemic administration of IMD-0354. Furthermore, IMD-0354 effectively reduced the levels of TNF-α and IL-1β in the lungs. These favorable results might be partly due to the use of a small compound with low molecular weight, not oligonucleotides. In fact, the molecular weight of IMD-0354 is low (383.7). It is likely that IMD-0354 is more easily delivered into lung tissue cells as compared with oligonucleotides, although we did not examine the concentration of IMD-0354 in the lung tissue.

On the other hand, the daily treatment of IMD-0354 throughout the experiments was required to exert the maximal antifibrotic effects because neither the early (Day 0 to 14) nor late (Day 15 to 28) treatment significantly prevented the pulmonary fibrosis induced by bleomycin. The reason for these results remains to be elucidated. Elevated activity of NF-κB was detected in the lung homogenates on Days 3 and 7 after bleomycin treatment in our system. However, the latent activity of NF-κB may have a role in the late phase of bleomycin-induced pulmonary fibrosis. Otherwise, the inhibitory activities for other kinases as well as biochemical actions of IMD-0354 are likely to be involved in the ability to attenuate bleomycin-induced pulmonary fibrosis. In particular, it is possible that IMD-0354 also has the antifibrotic, but not antiinflammatory, effects in the late phase of lung fibrogenesis. The direct effects of IMD-0354 on the growth and collagen production of lung fibroblasts are important targets of future experiments, since antiproliferative effects of IMD-0354 were recently reported (20). IMD-0354 may be a similar case to pirfenidone, which was originally developed as an antiinflammatory drug, but recently shown to have profound antifibrotic effects *in vitro* and in clinical trials for patients with IPF (29–31).

The analysis of BAL cells demonstrated that IMD-0354 reduced the number of accumulated neutrophils and lymphocytes on Day 7 and 14, respectively. The mechanism involved in inhibiting the accumulation of neutrophils by IMD-0354 is not clear. One possibility is that the inhibition of inflammatory cytokines in the lung, which are related to the activation of NF-κB, by IMD-0354 might contribute to reducing the accumulation of neutrophils and lymphocytes. Furthermore, we observed the reduction of macrophage inflammatory protein-2, which is known to be regulated by NF-κB and an important chemotactic factor for murine neutrophils, in the lungs treated with IMD-0354, although the difference did not reach a significant level (data not shown). Further studies regarding chemotactic factors to neutrophils and lymphocytes will be required.

A phase I study of IMD-0354 is now in progress. Recently, Onai and colleagues reported that IMD-0354 attenuated myocardial ischemia/reperfusion injury without general or cellular toxicity in rats (19). In our study, administration of IMD-0354 alone did not induce weight loss or any morphologic changes in the lungs. These results together with our data suggest that a novel IKKβ inhibitor, IMD-0354, might be useful for the treatment of patients with pulmonary fibrosis, especially which is related to the activation of NF-κB.

Conflict of Interest Statement: None of the authors have a financial relationship with a commercial entity that has an interest in the subject of this manuscript.

Acknowledgment: The authors thank Ms. Tomoko Oka for her technical assistance.

References

1. American Thoracic Society. Idiopathic pulmonary fibrosis: diagnosis and treatment. International consensus statement. *Am J Respir Crit Care Med* 2000;161:646–664.
2. Gross TJ, Hunninghake GW. Idiopathic pulmonary fibrosis. *N Engl J Med* 2001;345:517–525.
3. Selman M, King TE Jr, Pardo A. Idiopathic pulmonary fibrosis: prevailing and evolving hypotheses about its pathogenesis and implications for therapy. *Ann Intern Med* 2001;134:136–151.
4. American Thoracic Society. American Thoracic Society/European Respiratory Society international multidisciplinary consensus classification of the idiopathic interstitial pneumonias. *Am J Respir Crit Care Med* 2002;165:277–304.
5. Bouros D, Nicholson AC, Polychronopoulos V, du Bois RM. Acute interstitial pneumonia. *Eur Respir J* 2000;15:412–418.
6. Ware LB, Matthay MA. The acute respiratory distress syndrome. 2000;343:660–661.
7. Collard HR, King TE Jr. Demystifying idiopathic interstitial pneumonia. *Arch Intern Med* 2003;163:17–29.
8. Zhang XY, Shimura S, Masuda T, Saitoh H, Shirato K. Antisense oligonucleotides to NF-κB improve survival in bleomycin-induced pneumopathy of the mouse. *Am J Respir Crit Care Med* 2000;162:1561–1568.

9. Griesenbach U, Cassady RL, Cain RJ, duBois RM, Geddes DM, Alton EW. Cytoplasmic deposition of NFκB decoy oligonucleotides is insufficient to inhibit bleomycin-induced pulmonary inflammation. *Gene Ther* 2002;9:1109–1115.
10. Christman JW, Sadikot RT, Blackwell TS. The role of nuclear factor-κB in pulmonary diseases. *Chest* 2000;117:1482–1487.
11. Mercurio F, Zhu H, Murray BW, Shevchenko A, Bennett BL, Li JW, Young DB, Barbosa M, Mann M. IKK-1 and IKK-2: cytokine-activated IκB kinases essential for NK-κB activation. *Science* 1997;278:860–866.
12. Woronicz JD, Gao X, Cao Z, Rothe M, Goeddel DV. IκB kinase-β: NF-κB activation and complex formation with IκB kinase-A and NIK. *Science* 1997;278:866–869.
13. Takeda K, Takeuchi O, Tsujimura T, Itami S, Adachi O, Kawai T, Sanjo H, Yoshikawa K, Terada N, Akira S. Lim and skin abnormalities in mice lacking IKKα. *Science* 1999;284:271–273.
14. Hu Y, Baud V, Delhase M, Zhang P, Deerinck T, Ellisman M, Johnson R, Karin M. Abnormal morphogenesis but intact IKK activation in mice lacking the IKKα subunit of IκB kinase. *Science* 1999;284:316–320.
15. Li Q, Antwerp DV, Mercurio F, Lee K-F, Verma IM. Severe liver degeneration in mice lacking the IκB kinase 2 genae. *Science* 1999;284:321–325.
16. Conron M, Andreakos E, Pantelidis P, Smith C, Beynon HLC, Dubois RM, Foxwell BM. Nuclear factor-κB activation in alveolar macrophages require IκB kinase-β, but not nuclear factor-κB inducing kinase. *Am J Respir Crit Care Med* 2002;165:996–1004.
17. Inayama M, Nishioka Y, Makino H, Ugai M, Aono Y, Uehara H, Izumi K, Sone S. Antifibrotic effect of IKKβ inhibitor IMD-0354 in bleomycin-induced pulmonary fibrosis [abstract]. *Am J Respir Crit Care Med* 2005;171:A121.
18. Nishioka Y, Yano S, Fujiki F, Mukaida N, Matsushima K, Tsuruo T, Sone S. Combined therapy of multidrug-resistant human lung cancer with anti-P-glycoprotein antibody and monocyte chemoattractant protein-1 gene transduction:the possibility of immunological overcoming of multidrug resistance. *Int J Cancer* 1997;71:170–177.
19. Onai Y, Suzuki J, Kakuta T, Maejima Y, Haraguchi G, Fukasawa H, Muto S, Itai A, Isobe M. Inhibition of IkB phosphorylation in cardiomyocytes attenuates myocardial ischemia/reperfusion injury. *Cardiovasc Res* 2004;63:51–59.
20. Tanaka A, Konno M, Muto S, Kambe N, Morii E, Nakahata T, Itai A, Matsuda H. A novel NF-κB inhibitor, IMD-0354, suppresses neoplastic proliferation of human mast cells with constitutively activated c-*kit* receptors. *Blood* 2005;105:2324–2331.
21. Harrison JH, Lazo JS. High dose continuous infusion of bleomycin in mice: a new model for drug-induced pulmonary fibrosis. *J Pharmacol Exp Ther* 1987;243:1185–1194.
22. Aono Y, Nishioka Y, Inayama M, Ugai M, Kishi J, Uehara H, Izumi K, Sone S. Imatinib as a novel anti-fibrotic agent in bleomycin-induced pulmonary fibrosis in mice. *Am J Respir Crit Care Med* 2005;171:1279–1285.
23. Ashcroft T, Simpson JM, Timbrell V. Simple method of estimating severity of pulmonary fibrosis on a numerical scale. *J Clin Pathol* 1988;41:467–470.
24. Deryckere F, Gannon F. A one-hour minipreparation technique for extraction of DNA-binding proteins from animal tissues. *Biotechniques* 1994;16:405.
25. Renard P, Ernest I, Houbion A, Art M, Le Calvez H, Raes M, Remacle J. Development of a sensitive multi-well colorimetric assay for active NFkB. *Nucleic Acids Res* 2001;29:E21.
26. Jaffray C, Yang J, Carter G, Mendez C, Norman J. Pancreatic elastase activates pulmonary nuclear factor kappa B and inhibitory kappa B, mimicking pancreatitis-associated adult respiratory distress syndrome. *Surgery* 2000;128:225–231.
27. Newton R. Molecular mechanisms of glucocorticoid action: what is important? *Thorax* 2000;55:603–613.
28. Kirwan JR. Systemic glucocorticoids in rhematology. In: Hochberg MC, Silman AJ, Smolen JS, Weinblatt ME, Weisman MH, editors. Rheumatology, 3rd ed. Philadelphia: Elsevier Science; 2003, pp. 385–392.
29. Lurton JM, Trejo T, Narayanan AS, Raghu G. Pirfenidone inhibits the stimulatory effects of profibrotic cytokines on human lung fibroblasts *in vitro* [abstract]. *Am J Respir Crit Care Med* 1996;153:A403.
30. Raghu G, Johnson WC, Lockhart D, Mageto Y. Treatment of idiopathic pulmonary fibrosis with a new antifibrotic agent, pirfenidone: results of a prospective, open-label Phase II study. *Am J Respir Crit Care Med* 1999;159:1061–1069.
31. Azuma A, Nukiwa T, Tsuboi E, Suga M, Abe S, Nakata K, Taguchi Y, Nagai S, Itoh H, Ohi M, *et al.* Double-blind, placebo-controlled trial of pirfenidone in patients with idiopathic pulmonary fibrosis. *Am J Respir Crit Care Med* 2005;171:1040–1047.

Clinical and Experimental Immunology ORIGINAL ARTICLE doi:10.1111/j.1365-2249.2007.03423.x

CXCL9 and 11 in patients with pulmonary sarcoidosis: a role of alveolar macrophages

Y. Nishioka, K. Manabe, J. Kishi, W. Wang, M. Inayama, M. Azuma and S. Sone

Department of Internal Medicine and Molecular Therapeutics, Institute of Health Biosciences, University of Tokushima Graduate School, Tokushima, Japan

Accepted for publication 30 April 2007

Correspondence: Yasuhiko Nishioka MD, Department of Internal Medicine and Molecular Therapeutics, Institute of Health Biosciences, University of Tokushima Graduate School, 3-18-15 Kuramoto-cho, Tokushima 770–8503, Japan.
E-mail: yasuhiko@clin.med.tokushima-u.ac.jp

Summary

Interferon-inducible protein-10 (IP-10)/CXCL10, which is a ligand for CXC chemokine receptor 3 (CXCR3), is known to be involved in the pathogenesis of pulmonary sarcoidosis. However, the roles of monokine induced by interferon γ (Mig)/CXCL9 and interferon-inducible T cell α chemoattractant (I-TAC)/CXCL11, which are also CXCR3 ligands, remain unclear. Mig/CXCL9, IP-10/CXCL10 and I-TAC/CXCL11 in both bronchoalveolar lavage fluid (BALF) and serum in patients with pulmonary sarcoidosis were measured by enzyme-linked immunosorbent assay (ELISA). The expression of these chemokines in alveolar macrophages was examined using ELISA, quantitative real-time polymerase chain reaction and immunostaining. In BALF, Mig/CXCL9 and IP-10/CXCL10 were significantly elevated in stage II sarcoidosis as compared with the levels in healthy volunteers. In serum, Mig/CXCL9 and I-TAC/CXCL11 were increased in stage II of the disease. The levels of all CXCR3 ligands in BALF were correlated with the numbers of both total and $CD4^+$ lymphocytes. Alveolar macrophages were stained positive for all CXCR3 ligands and produced increased amounts of these chemokines. Positive staining of the three chemokines was also observed in the epithelioid and giant cells in the sarcoid lungs. These findings suggest that Mig/CXCL9 and I-TAC/CXCL11 as well as IP-10/CXCL10 play important roles in the accumulation of Th1 lymphocytes in sarcoid lungs.

Keywords: alveolar macrophages, CXCL9, CXCL10, CXCL11, sarcoidosis

Introduction

Sarcoidosis is a systemic granulomatous disease of unknown cause that mainly affects the lung and lymphatic system of the body [1–4]. Although spontaneous remission occurs in nearly two-thirds of patients, chronic and progressive courses are observed in 10–30% of patients [1,2]. The sarcoid granuloma is characterized by non-caseating epithelioid cells with the dominant accumulation of $CD4^+$ T cells and macrophages [1–4].

$CD4^+$ T lymphocytes are divided into two subgroups, T helper (Th) 1 and Th2 cells, on the basis of their cytokine production [5]. Based on the Th1/Th2 paradigm, sarcoidosis is considered to be a typical Th1-dominant disease, as T lymphocytes in bronchoalveolar lavage fluid (BALF) and lymph nodes from sarcoidosis preferentially produce interferon (IFN)-γ, interleukin (IL)-2 and tumour necrosis factor (TNF)-α or β [6–8]. Recently, the chemokine receptors expressed specifically on Th1 or Th2 cells were identified, and it was reported that Th1 cells are characterized by the expression of CCR5 or CXCR3, and Th2 cells by CCR4 expression [9]. BAL lymphocytes in sarcoidosis have been reported to be highly positive for CCR5 and CXCR3 [10–12]. In particular, CXCR3 is expressed on more than 97% (88·6–99·2%) of BAL $CD4^+$ T cells in sarcoidosis, while CCR5 is expressed on 50·5% (30·5–81·2%) [12]. Therefore, the analysis of CXCR3 ligands in sarcoidosis is of importance to clarify the mechanisms of accumulation of Th1 cells into the sarcoid lungs. Interferon-inducible protein-10 (IP-10)/CXCL10, which is one of the CXCR3 ligands, was reported to be elevated in BALF of patients with sarcoidosis and to play crucial roles in the Th1-immune response in the sarcoid lungs [11,13]. Alveolar macrophages and epithelioid cells are known to be the main producers of IP-10/CXCL10 [13]. However, the roles of other CXCR3 ligands, monokine induced by interferon γ (Mig)/CXCL9 and interferon-inducible T cell α-chemoattractant (I-TAC)/CXCL11, in the pathogenesis of sarcoidosis, still remain unclear. We therefore examined the levels of Mig/CXCL9 and I-TAC/CXCL11 as well as IP-10/CXCL10 in BALF and serum in patients with

Table 1. Characteristics of study population.

Group	Male/female	Age (years)	Total cells ($\times 10^5$/ml)	Bronchoalveolar lavage % Total cells AM	Ly	Neut	Eo	$CD4^+/CD8^+$
HV	8/1	23·7 ± 2·1	1·6 ± 0·2	87·9 ± 2·7	9·8 ± 2·0	1·8 ± 1·3	0·4 ± 0·1	n.d.
Sar	18/26	49·1 ± 13·3	2·4 ± 0·3*	71·0 ± 2·3†	27·1 ± 2·2†	1·1 ± 0·4	0·7 ± 0·3	5·25 ± 0·5

AM = alveolar macrophages; Eo = eosinophils; HV = healthy volunteers; Ly = lymphocytes; Neut = neutrophils; n.d. = not determined; Sar = sarcoidosis.

Data are shown as mean ± standard error of the mean. *$P < 0.05$, compared with the group of healthy volunteers. †$P < 0.001$, compared with the group of healthy volunteers.

different stages of sarcoidosis and the expressions of these chemokines in alveolar macrophages.

Methods

Subjects

Studies were performed in 44 patients with sarcoidosis and nine healthy volunteers (HV) (Table 1). Sarcoidosis was diagnosed according to previously described clinical and histological criteria [1]. Based on chest radiography, patients were subdivided into four stages (stage 0: $n = 10$, stage I; $n = 18$, stage II: $n = 12$, stages III and IV: $n = 4$). Ten patients with normal chest X-ray findings (stage 0) had positive biopsy findings of the lung or skin and uveitis. None of the patients were receiving corticosteroid therapy at the time of the investigation. None of the HV showed any abnormalities on physical examinations, chest X-ray and lung function tests. The study was approved by the ethics committee of the University of Tokushima and written informed consent was obtained from the subjects.

Bronchoalveolar lavage

BAL was performed as described previously [14,15]. Briefly, a flexible fibreoptic bronchoscope (Model 1T20; Olympus Co., Tokyo, Japan) was wedged into a segmental or subsegmental bronchus of the middle lobe or lingula, and lavage was performed with a total volume of 150 ml of sterile 0·9% saline warmed at 37°C in three 50-ml aliquots. The fluid recovered was passed through the sterile gauze and the supernatants were stored at −80°C until examination. The total number of cells was counted using the trypan-blue dye exclusion test. Differential counts on 400 cells were carried out on smears of sedimented cells stained with Diff-Quik stain (Baxter Dade AG, Duedingen, Switzerland) [14,15]. Blood samples were collected at the time of diagnosis.

Measurement of CXCR3 ligands by enzyme-linked immunosorbent assay (ELISA)

The frozen BALF was thawed quickly and used to examine the concentration of three CXCR3 ligands by ELISA (R&D System, Minneapolis, MN, USA) [15,16]. The minimal detectable level of Mig/CXCL9 was 3·84 pg/ml, and those of IP-10/CXCL10 and I-TAC/CXCL11 were 1·67 pg/ml.

Harvesting of the supernatant of alveolar macrophages

BAL cells were added to a 96-well flat-bottomed plate at 1×10^5 of alveolar macrophages per well in triplicate cultures [15]. These cells were washed with cold phosphate-buffered saline (PBS) to remove the non-adherent cells. The purity of alveolar macrophages at this point was more than 90%. More than 93% were viable as judged by the trypan blue dye exclusion test. Cells were subsequently cultured in RPMI-1640 supplemented with 10% heat-inactivated fetal bovine serum (FBS; Gibco, Grand Island, NY, USA). Their supernatants were harvested after culture for 24 and 48 h.

Preparation of total RNA of alveolar macrophages

Total RNA was isolated from alveolar macrophages using Isogen (Wako KK, Kyoto, Japan) as described previously [15]. Briefly, 1 ml of Isogen was added to the culture of alveolar macrophages in a 10-cm dish, and then the cells were harvested into an Eppendorf tube using a cell-scraper (Sumitomo Bakelite Co., Ltd, Tokyo, Japan). Total RNA was extracted according to the manufacturer's instructions [15].

Real-time quantitative polymerase chain reaction (PCR) analysis for CXCR3 ligands

Ten nanograms of total RNA were used for RT–PCR using a one-step real-time PCR kit (Applied Biosystems, Foster City, CA, USA). Real-time quantitative PCR was performed using an ABI prism 7700 Sequence detector (Applied Biosystems) [15]. The primers and probes for human CXCR3 ligands were designed based on published sequence data [17–19], and were as follows: Mig/CXCL9 forward primer, 5′-CCAAGGGA CTATCCACCTACAATC-3′; Mig/CXCL9 reverse primer, 5′-GGTTTAGACATGTTTGAACTCCATTC-3′; Mig/CXCL9 *Taq*Man probe, 5′-FAM-CCTTAAACAATTTGCCCCAAG CCCTTC-TAMRA-3′: IP-10/CXCL10 forward primer,

5′-CTGACTCTAAGTGGCATTCAAGGA-3′; IP-10/CXCL10 reverse primer, 5′-CAATGATCTCAACACGTGGACAA-3′; IP-10/CXCL10 *Taq*Man probe, 5′-FAM-AGAACCGTAC GCTGTACCTGCATCAGCA-TAMRA-3′: I-TAC/CXCL11 forward primer, 5′-GGGTACATTATGGAGGCTTTCT CA-3′; I-TAC/CXCL11 reverse primer, 5′-GAGGACGC TGTCTTTGCATAGG-3′; and I-TAC/CXCL11 *Taq*Man probe, 5′-FAM-TCTGCCACTTTCACTGCTTTTACCCCA-TAMRA-3′. Each RT–PCR reaction was performed in duplicate wells using a *Taq*Man one-step RT–PCR Master Mix Reagents Kit (Applied Biosystems). The RT reaction was performed at 48°C for 30 min and 95°C for 10 min. PCR was performed for 40 cycles at 95°C for 15 s and 60°C for 1 min. Real-time RT–PCR for β-actin was also performed as a control using *Taq*Man β-actin Control Reagents (Applied Biosystems) under the same conditions as for the three CXCR3 ligands. The relative expression level of each CXCR3 ligand mRNA was calculated as the value of CXCR3 ligand mRNA/the value of β-actin mRNA [15].

Immunofluorescence staining

Immmunofluorescence staining was performed as described previously [20]. BAL cells were cytocentrifuged onto glass slides and fixed in cold acetone for 10 min, and were stained with rabbit anti-human Mig/CXCL9, IP-10/CXCL10 or I-TAC/CXCL11 polyclonal antibodies (PeproTech EC Ltd, London, UK) and Alexa fluor 488-conjugated goat anti-rabbit IgG (H + L) antibody (Molecular Probes, Eugene, OR, USA). These slides were mounted with Vectashield mounting medium containing 4′, 6 diamidino-2-phenylindole (DAPI) (Vector Laboratories, Inc., Burlingame, CA, USA), and visualized using a fluorescence microscope (Olympus BX61; Olympus Optical Co. Ltd, Tokyo, Japan).

Immunohistochemistry

Fresh frozen lung tissues were obtained from patients with sarcoidosis by lung biopsy at video-assisted thoracic surgery. Fragments of the tissues were covered with Tissue-Tek optimal cutting temperature (OCT) compound (Ames, Elkhart, IN, USA), snap-frozen in liquid nitrogen, and stored at −80°C until analysed. Six-micron sections were dried and fixed in cold acetone for 10 min. Staining was performed using the RTU Vectastain Universal Quick Kit (Vector Laboratories) [21,22]. The sections were incubated in 3% H_2O_2 in methanol for 30 min to inhibit endogenous peroxidase, and incubated in blocking serum for 10 min. The slides were then incubated overnight with rabbit anti-human Mig/CXCL9, IP-10/CXCL10 or I-TAC/CXCL11 polyclonal antibodies (PeproTech) at 4°C. After washing, sections were incubated in prediluted biotinylated panspecific universal secondary antibody for 10 min, followed by incubation in ready-to-use streptavidin/peroxidase complex reagent for 5 min. Sections were developed with a diaminobenzidine substrate kit (Vector Laboratories, Inc.) and counterstained with Mayer's haematoxylin (Muto Pure Chemicals Co., Ltd, Tokyo, Japan).

Statistical analysis

Comparisons among multiple groups were analysed using the one-way analysis of variance (ANOVA) with Newman–Keuls *post-hoc* correction (GraphPad Prism, version 3·0). Statistical analysis between two groups was performed using the unpaired two-tailed Student's *t*-test. Correlation coefficients were determined using the Pearson's linear regression analysis in StatView software. Differences were considered significant when *P*-values were less than 0·05.

Results

Characteristics of BALF of patients with sarcoidosis

The characteristics of the BALF of patients with sarcoidosis and BALF of healthy volunteers (HV) are shown in Table 1. The total number of cells in the BALF of patients with sarcoidosis was significantly higher than that in the BALF of HV ($P < 0·05$). The percentage of lymphocytes was increased significantly in sarcoidosis patients compared with HV ($P < 0·001$).

Concentrations of CXCR3 ligands, Mig/CXCL9, IP-10/CXCL10 and I-TAC/CXCL11 in BALF and serum of patients with sarcoidosis

We examined the levels of Mig/CXCL9, IP-10/CXCL10 and I-TAC/CXCL11 in both the BALF and serum of patients with sarcoidosis using ELISA. The results are shown in Fig. 1. In BALF, Mig/CXCL9 and IP-10/CXCL10 tended to be higher in patients at all stages of sarcoidosis, and were significantly elevated in stage II sarcoidosis compared with that of HV ($P < 0·05$). The level of I-TAC/CXCL11 in BALF was too low to detect in most samples, although in some samples from stage II sarcoidosis and HV I-TAC/CXCL11 was present at a detectable level. In serum, Mig/CXCL9 and I-TAC/CXCL11 tended to be higher in patients at all stages of sarcoidosis, and were elevated significantly in stage II sarcoidosis compared with HV (Mig/CXCL9: $P < 0·05$, I-TAC/CXCL11: $P < 0·01$). However, there was no difference in serum IP-10/CXCL10 among all stages of sarcoidosis and HV.

Relationship between the level of each CXCR3 ligand (Mig/CXCL9, IP-10/CXCL10 and I-TAC/CXCL11) and the number of lymphocytes in BALF of patients with sarcoidosis

We examined the correlations between the level of each CXCR3 ligand and the number of lymphocytes in the BALF of patients with sarcoidosis. As shown in Fig. 2, there was a positive correlation between the concentration of Mig/

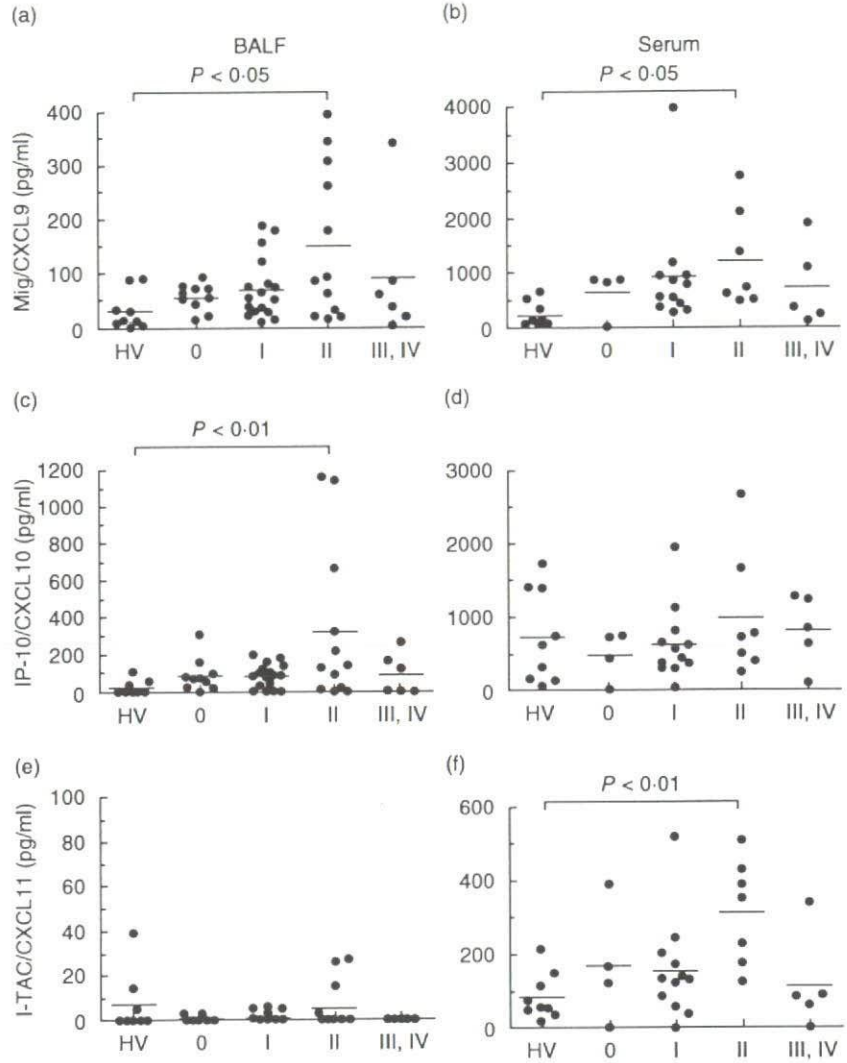

Fig. 1. Concentrations of monokine induced by interferon γ(Mig)/CXCL9, interferon-inducible protein-10 (IP-10)/CXCL10 and interferon-inducible T cell α-chemoattractant (I-TAC)/CXCL11 in both bronchoalveolar lavage fluid (BALF) and serum of patients with sarcoidosis and healthy subjects. The BALF harvested from healthy volunteers (HV) or patients with various stages of sarcoidosis were used for the measurement of CXCR3 ligands by enzyme-linked immunosorbent assay (ELISA). Each closed circle indicates an individual specimen. A value of 0 (pg/ml) was given to all samples that read out below the level of detection in the ELISA.

CXCL9, IP-10/CXCL10 and I-TAC/CXCL11 and the number of lymphocytes (Mig/CXCL9: $r = 0{\cdot}495$, $P = 0{\cdot}0006$; IP-10/CXCL10: $r = 0{\cdot}716$, $P < 0{\cdot}0001$; I-TAC/CXCL11: $r = 0{\cdot}760$, $P < 0{\cdot}001$). When we analysed the correlation between the number of $CD4^+$ lymphocytes and the level of each CXCR3 ligand in BALF, higher correlations than those between total lymphocytes and each CXCR3 ligand were observed (Mig/CXCL9: $r = 0{\cdot}537$, $P = 0{\cdot}0001$; IP-10/CXCL10: $r = 0{\cdot}743$, $P < 0{\cdot}0001$; I-TAC/CXCL11: $r = 0{\cdot}793$, $P < 0{\cdot}0001$).

Relationship among the levels of Mig/CXCL9, IP-10/CXCL10 and I-TAC/CXCL11 in patients with sarcoidosis

We next examined the correlations between the levels of each CXCR3 ligand in BALF and those in serum in patients with sarcoidosis. There were significant correlations between the BALF and serum levels of each CXCR3 ligand (Mig/CXCL9: $r = 0{\cdot}569$, $P = 0{\cdot}002$; IP-10/CXCL10: $r = 0{\cdot}639$, $P = 0{\cdot}0003$; I-TAC/CXCL11: $r = 0{\cdot}501$, $P = 0{\cdot}0082$).

Furthermore, high correlations among the levels of the three CXCR3 ligands in both BALF and serum were observed (Mig/CXCL9 and IP-10/CXCL10: BALF; $r = 0{\cdot}657$, $P < 0{\cdot}0001$, serum; $r = 0{\cdot}688$, $P < 0{\cdot}0001$; IP-10/CXCL10 and I-TAC/CXCL11: BALF; $r = 0{\cdot}876$, $P < 0{\cdot}0001$, serum; $r = 0{\cdot}741$, $P < 0{\cdot}0001$; I-TAC/CXCL11 and Mig/CXCL9: BALF; $r = 0{\cdot}664$, $P < 0{\cdot}0001$, serum; $r = 0{\cdot}749$, $P < 0{\cdot}0001$) (Fig. 3).

Immunostaining of Mig/CXCL9, IP-10/CXCL10 and I-TAC/CXCL11 in BAL cells and lung tissue in sarcoidosis

To analyse which cells produce Mig/CXCL9, IP-10/CXCL10 and I-TAC/CXCL11 in the sarcoid lungs, we performed the immunostaining of both BAL cells and lung tissues. Immunofluorescent staining of BAL cells showed that alveolar macrophages, but not lymphocytes, were positive for all CXCR3 ligands (Fig. 4). In particular, I-TAC/CXCL11 was stained strongly when compared with Mig/CXCL9 and

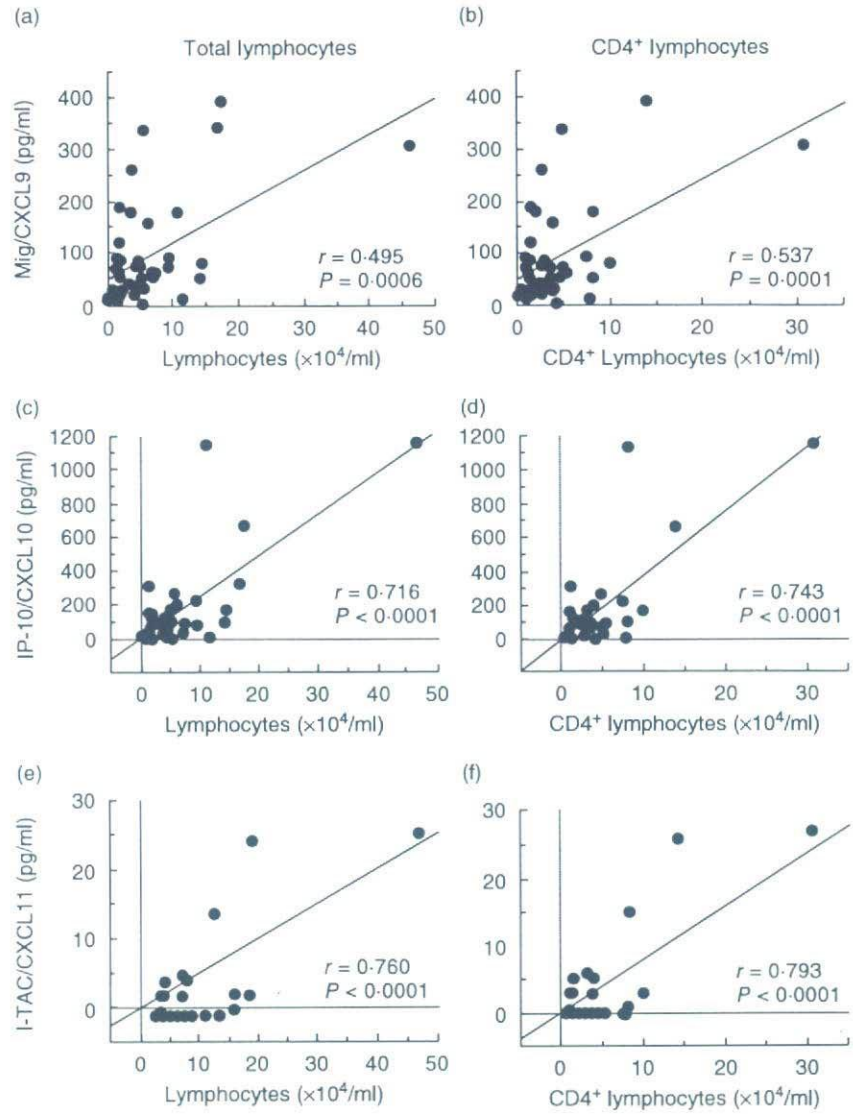

Fig. 2. Correlation between the level of each CXCR3 ligand and the number of total or $CD4^+$ lymphocytes in bronchoalveolar lavage fluid (BALF). The correlations between the level of each CXCR3 ligand and the number of lymphocytes (a, c, e) or $CD4^+$ lymphocytes (b, d, f) in the BALF of patients with sarcoidosis was examined.

IP-10/CXCL10. All CXCR3 ligands were also stained in epithelioid and giant cells in sarcoid granuloma in immunohistochemical analysis. Again, macrophages in the alveolar lumens were positive for all three CXCR3 ligands.

Increased production of Mig/CXCL9, IP-10/CXCL10 and I-TAC/CXCL11 by alveolar macrophages from patients with sarcoidosis

Immunostaining showed that alveolar macrophages are one of the crucial producers of CXCR3 ligands. We therefore examined the production of CXCR3 ligands by alveolar macrophages harvested from HV and patients with sarcoidosis. Alveolar macrophages harvested from patients with sarcoidosis had the ability to spontaneously produce a higher amount of all CXCR3 ligands compared with those from HV (Fig. 5). Alveolar macrophages from patients with sarcoidosis also expressed higher amounts of mRNAs of all CXCR3 ligands than those from HV (Fig. 5).

Discussion

In the present study, we examined the levels of Mig/CXCL9 and I-TAC/CXCL11 as well as IP-10/CXCL10 in BALF and serum in patients with different stages of sarcoidosis. IP-10/CXCL10, which is one of the CXCR3 ligands, has been reported to play crucial roles in Th1-immune responses in sarcoid lungs [11,13]. However, three ligands for CXCR3 including Mig/CXCL9, IP-10/CXCL10 and I-TAC/CXCL11, have been identified [9]. In fact, co-expression of these chemokines in the lungs has been reported in mouse [23,24] as well as in humans [25]. In addition, there are some differences in the levels and time-courses of expression of these CXCR3 ligands [23–25]. These findings prompted us to

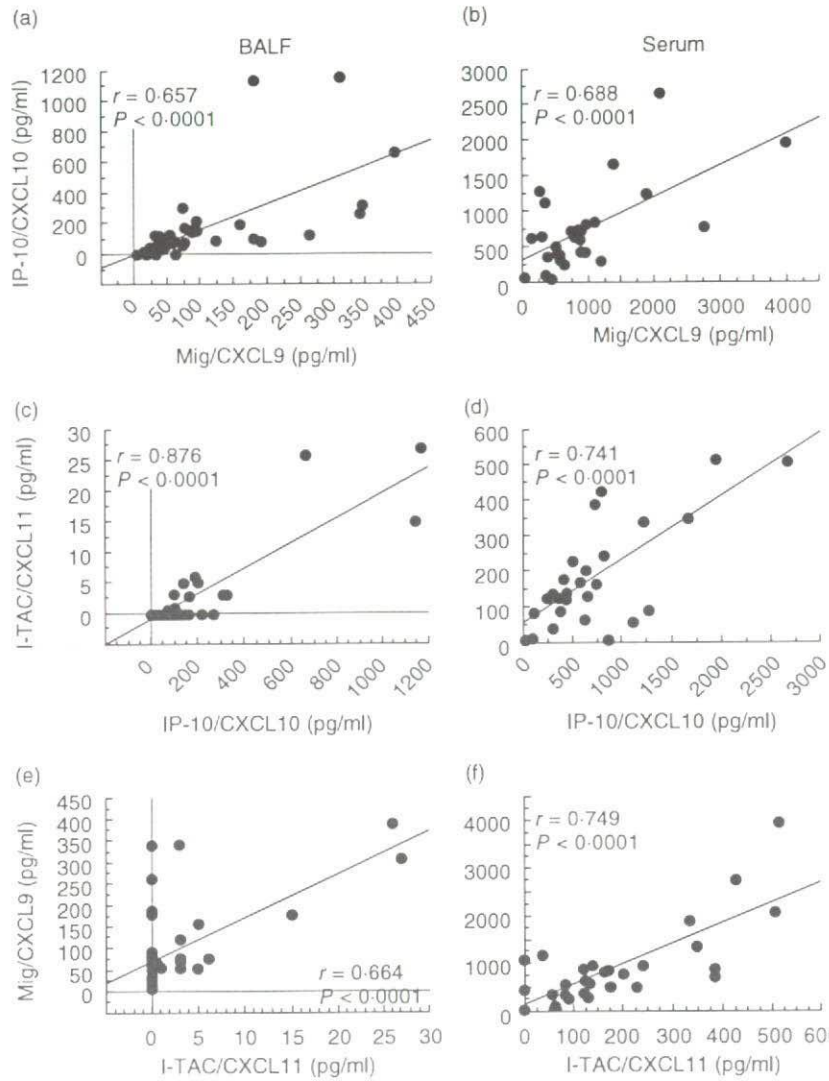

Fig. 3. Correlation among the levels of three CXCR3 ligands in bronchoalveolar lavage fluid (BALF) and serum. The correlations between the levels of each CXCR3 ligand in BALF (a, c, e) and those in serum (b, d, f) in patients with sarcoidosis.

study the expressions of Mig/CXCL9 and I-TAC/CXCL11 in sarcoidosis. We observed the same levels of Mig/CXCL9 as of IP-10/CXCL10 in BALF, whereas the concentration of I-TAC/CXCL11 was below the detectable level in most cases. More recently, Pignatti *et al.* studied the BAL fluid of eight patients with sarcoidosis and was not able to detect the expression of I-TAC/CXCL11 [26]. Our results seem to be consistent with their report.

On the other hand, the concentration of I-TAC/CXCL11 in serum was detectable but low, being average one-tenth of the levels of Mig/CXCL9 and IP-10/CXCL10. Interestingly, no significant difference was found among the concentrations at the various stages of sarcoidosis and HV for serum IP-10/CXCL10, although Mig/CXCL9 and I-TAC/CXCL11 were elevated at stage II of sarcoidosis. The reason for this is not clear, but IP-10/CXCL10 is likely to increase at various

Fig. 4. Immunostaining of monokine induced by interferon γ (Mig)/CXCL9, interferon-inducible protein-10 (IP-10)/CXCL10 and interferon-inducible T cell α-chemoattractant (I-TAC)/CXCL11 in bronchoalveolar lavage (BA) cells and sarcoid lungs. BAL cells were cytocentrifuged on glass slides and fixed. The slides were incubated with control rabbit serum (a), anti-Mig/CXCL9 (b), IP-10/CXCL10 (c) or I-TAC/CXCL11 antibody (d), and stained with Alexa fluor 488-conjugated goat anti-rabbit IgG (H + l) antibody (green fluorescence) and 4′,6 diamidino-2-phenylindole (DAPI; by which nuclei were counterstained) (blue). Immunostaining was visualized using a fluorescence microscope (original magnifications: × 400). Arrows point to the lymphocytes which are negative for CXCR3 ligands. Freshly frozen lung sections derived from three patients with stage II of sarcoidosis were also stained with control rabbit serum (e), anti-Mig/CXCL9 (f), IP-10/CXCL10 (g) or I-TAC/CXCL11 antibody (h) and RTU Vectastain Universal Quick Kit, and developed with diaminobenzidine (DAB) substrate (original magnifications: × 200). The insets in e, f, g and h show the staining of macrophages in the alveolar lumen (original magnifications: × 400). Scale bars = 50 μm.

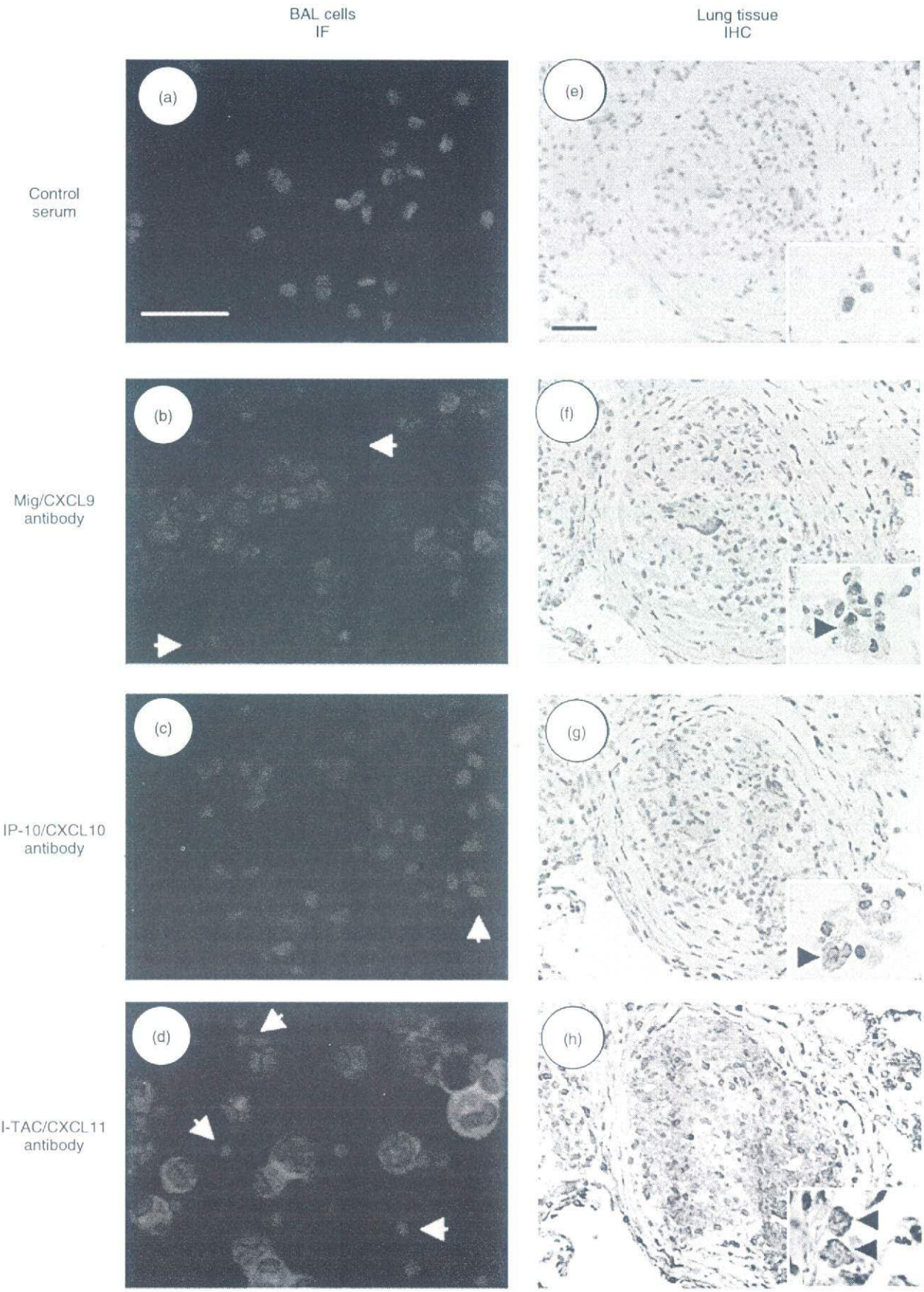
BAL cells
IF
Lung tissue
IHC
Control serum
Mig/CXCL9 antibody
IP-10/CXCL10 antibody
I-TAC/CXCL11 antibody
(a)
(b)
(c)
(d)
(e)
(f)
(g)
(h)